Atmos. Chem. Phys. Discuss., https://doi.org/10.5194/acp-2018-984
Manuscript under review for journal Atmos. Chem. Phys.
Discussion started: 4 October 2018

Atmospheric Chemistry and Physics Discussions
Open Access

Top-down estimate of black carbon emissions for city cluster using ground observations: A case study in southern Jiangsu, China

Xuefen Zhao[1], Yu Zhao[1, 2*], Dong Chen[1], Chunyan Li[3], Jie Zhang[3]

1. State Key Laboratory of Pollution Control and Resource Reuse and School of the Environment, Nanjing University, 163 Xianlin Ave., Nanjing, Jiangsu 210023, China

2. Jiangsu Collaborative Innovation Center of Atmospheric Environment and Equipment Technology (CICAEET), Nanjing University of Information Science and Technology, Jiangsu 210044, China

3. Jiangsu Provincial Academy of Environmental Science, 176 North Jiangdong Rd., Nanjing, Jiangsu 210036, China

*Corresponding author: Yu Zhao

Phone: 86-25-89680650; email: yuzhao@nju.edu.cn

Atmos. Chem. Phys. Discuss., https://doi.org/10.5194/acp-2018-984
Manuscript under review for journal Atmos. Chem. Phys.
Discussion started: 4 October 2018

Atmospheric Chemistry and Physics Discussions

Abstract

We combined a chemistry transport model (CTM), a multiple regression model and available ground observations, to derive top-down estimate of black carbon (BC) emissions and to reduce deviations between simulations and observations for southern Jiangsu city cluster, a typical developed region of eastern China. Scaled from a high-resolution inventory for 2012 based on changes in activity levels, the BC emissions in southern Jiangsu were calculated at 27.0 Gg/yr for 2015 (JS-prior). The annual mean concentration of BC at Xianlin Campus of Nanjing University (NJU, a suburban site) was simulated at 3.4 μg/m^3, 11% lower than the observed 3.8 μg/m^3. In contrast, it was simulated at 3.4 μg/m^3 at Jiangsu Provincial Academy of Environmental Science (PAES, an urban site), 36% higher than the observed 2.5 μg/m^3. The discrepancies at the two sites implied the uncertainty of the bottom-up inventory of BC emissions. Assuming a near-linear response of BC concentrations to emission changes, we applied a multiple regression model to fit the hourly surface concentrations of BC at the two sites, based on the detailed source contributions to ambient BC levels from brute-force simulation. Constrained with this top-down method, BC emissions were estimated at 13.4 Gg/yr (JS-posterior), 50% smaller than the bottom-up estimate, and stronger seasonal variations were found. Biases between simulations and observations were reduced for most months at the two sites when JS-posterior was applied. At PAES, in particular, the simulated annual mean was elevated to 2.6 μg/m^3 and the annual normalized mean error (NME) decreased from 72.0% to 57.6%. However, application of JS-posterior slightly enhanced NMEs in July and October at NJU where simulated concentrations with JS-prior were lower than observations, implying that reduction in total emissions could not correct CTM underestimation. The effects of numbers and spatial representativeness of observation sites on top-down estimate were further quantified. The best CTM performance was obtained when observations of both sites were used with their difference in spatial functions considered in emission constraining. Given the limited BC observation data

in the area, therefore, more measurements with better spatiotemporal coverage were recommended for constraining BC emissions effectively. Top-down estimates derived from JS-prior and the Multi-resolution Emission Inventory for China (MEIC) were compared to test the sensitivity of the method to initial emission input. The differences in emission levels, spatial distributions and CTM performances were largely reduced after constraining, implying that the impact of initial inventory was limited on top-down estimate. Sensitivity analysis proved the rationality of near linearity assumption between emissions and concentrations, and the impact of wet deposition on the multiple regression model was demonstrated moderate through data screening based on simulated wet deposition and satellite-derived precipitation.

1 Introduction

Black carbon (BC), alternatively referred as elemental carbon (EC), is an crucial component of atmospheric particle and comes mainly from incomplete combustion of fossil fuels and biomass. BC has adverse effect on human health as it absorbs harmful volatile organic compounds like polycyclic aromatic hydrocarbons (Dachs and Eisenreich, 2000). Furthermore, BC contributes to global warming by intercepting and absorbing sunlight (Jacobson, 2001; Ramanathan and Carmichael, 2008). Bond et al. (2013) assessed that the global average radiative forcing of BC was +1.1 W/m^2 (90% confidence interval: 0.17-2.1 W/m^2), which was more than two-thirds of that from CO_2 (+1.56 W/m^2). Since BC remains for only a few days in the atmosphere, it is an effective way to mitigate climate warming in the short term by reducing BC emissions. However, due to lack of sufficient understanding of major emission sources, the effect of BC on regional climate was not fully quantified by models.

BC emission inventories are traditionally developed with the bottom-up method based on activity levels and emission factors. Previous studies of chemistry transport modeling (CTM) based on emission inventories found large discrepancies between simulated and observed BC concentrations. Koch et al. (2009) found that sixteen models applied in the AeroCom aerosol model inter-comparison project underestimated surface BC levels by a factor of 2-3. Hu et al. (2016) found that CTM significantly underestimated the peak surface concentrations of BC over northwestern United States, likely due to missing strong local fire events in fire emissions. Moreover, large differences existed in various bottom-up emission inventories, particularly for China with large energy consumption, complicated emission source categories, and fast changes in emission characteristics. BC emissions in China for 2001 and 2006 in the Regional Emission inventory in ASia (REAS 2.1, Kurokawa et al., 2013) were smaller than those in the Intercontinental Chemical Transport Experiment-Phase B (INTEX-B, Zhang et al., 2009), but the growth rate of BC emissions in REAS 2.1 was larger than that in INTEX-B (30% versus 15%) for the five years. Ohara et al. (2007) evaluated the inter-annual trend in China's BC emissions with constant emission factors, and found that the national emissions continuously decreased by 23% from 1990 to 2000. In contrast, Lei et al. (2011) suggested a much smaller inter-annual variability with the peak annual emissions found in 1996 for the same period. The differences resulted largely from the use of activity levels from various data sources, especially for residential biofuel combustion. The gaps between different studies implied potentially large uncertainties in BC bottom-up emission inventories. The uncertainties of BC emission estimates for China were reported at ±484%, ±208%, and ±98% by Streets et al. (2003), Zhang et al. (2009), and Lu et al. (2011), respectively. Due to lack of sufficient local field tests, emission factors were commonly taken from foreign studies with big variety depending on fuel and combustion condition (Bond et al., 2004; Cao et al., 2006; Lei et al., 2011; Qin and Xie, 2012; Streets et al., 2003; Streets et al., 2001; Zhang et al., 2009). It was also difficult to obtain accurate and detailed activity data, particularly for the main sources of BC including small industries (e.g., coke and brick production), off-road transportation, and residential solid fuel combustion. Besides the large uncertainty in emission estimation, challenges existed as well in updating BC inventories continuously (Hong et al., 2017; Lu et al., 2011; Xia et al., 2016; Zhao et

Atmos. Chem. Phys. Discuss., https://doi.org/10.5194/acp-2018-984
Manuscript under review for journal Atmos. Chem. Phys.
Discussion started: 4 October 2018

Atmospheric Chemistry and Physics Discussions

al., 2013). To beat severe air pollution, China has been conducting series of measures in energy conservation and emission control, leading to dramatic changes in energy structure, emission factors and removal rates of air pollutant control devices (Zhao et al., 2014). Such changes could be partly tracked by continuous emission monitoring system (CEMS) that was commonly installed at big industrial enterprises. Large fractions of BC emissions, however, came from medium and small sources, and their most recent improvements in manufacturing technologies and emission controls were relatively difficult to be obtained timely and efficiently.

Given above limitations in bottom-up inventories, different top-down approaches were applied to evaluate BC emissions. For example, Cohen and Wang (2014) presented a Kalman filter technique to estimate the global BC emissions based on satellite-derived radiances and surface concentrations from global and regional networks. The adjoint-based 4-D variational approach was also applied to constrain the bottom-up BC emissions at the global or national scales (Zhang et al., 2015; Xu et al., 2013; Guerrette et al., 2017). A near-linear response of BC concentrations to emission changes was generally assumed at national (Fu et al., 2012; Kondo et al., 2011; Wang et al., 2013) and regional scales (Li et al., 2015; Wang et al., 2011), due to its weak activity in atmospheric chemistry reaction. The ratio of observed to simulated concentration can be used as a scaling factor to correct BC emissions. Kondo et al. (2011) made continuous measurement of BC concentrations for a full year on a remote island in East China Sea. With the data strongly affected by emissions from China identified and those largely influenced by wet deposition excluded, they estimated China's annual anthropogenic BC emissions at 1.92 TgC/yr. Wang et al. (2013) verified this linearity by conducting sensitivity simulation in which emissions were increased by 50%. After excluding observation data of heavy pollution and strong precipitation events at five Chinese sites, they calculated China's annual BC emissions at 1.80 TgC/yr. The results of both studies were close to a bottom-up estimate at 1.81 TgC/yr by Zhang et al. (2009). Based on observations at

10 Chinese background and rural sites, Fu et al. (2012) applied a multiple regression model and CTM to quantify China's BC emissions. They calculated the total emissions at 3.05 TgC/yr, 59% larger than those by Zhang et al. (2009). Using similar approach, Li et al. (2015) estimated BC emissions to be 34% larger than bottom-up inventory in Pearl River Delta in south China by Zheng et al. (2012). Park et al. (2003) used the multiple linear regression to fit the Interagency Monitoring of Protected Visual Environments (IMPROVE) data and estimated that BC emissions from fossil fuel and biofuel burning in the United States should be increased by 15%. Combining a general circulation model simulation and the receptor modeling approach, Verma et al. (2017) constrained BC emissions over India based on the scaling factor (the ratio of simulated to observed BC concentration).

To our knowledge, limitations remained in the assessment of BC emissions based on the top-down approach. Current available studies focused mainly on global or national scale, and few evaluations could be found for city clusters. In aims of examining emission control policies and quantifying impacts of BC on local climate and air quality, there was a strong need for studies at city cluster scale that require ground observation and emission inventory with improved details. Regarding measurement data, monthly or annual means were commonly used in previous studies, and information of heavy-polluted events were lost when targeting a local scale. In general, observations at a higher temporal resolution were considered as an important means to effectively reduce uncertainties (Matsui et al., 2013; Wang et al., 2013; Gilardoni et al., 2011). Moreover, it was somewhat arbitrary to differentiate emissions by sector in previous top-down estimates, attributed to lack of detailed information on source categories from bottom-up inventories. The method was thus insufficient to make substantial improvement on emission evaluation by sector, or to clearly stress the direction of further revisions on bottom-up inventories.

In this work, therefore, we integrated CTM, multiple regression model and available hourly ground observations to provide top-down constraint of BC emissions and to reduce deviations between simulations and observations at city cluster scale. We selected southern Jiangsu city cluster including cities of Suzhou, Wuxi, Changzhou, Zhenjiang, and Nanjing, a typical region with large population and economy in Yangtze River Delta (YRD), China (see the geographic location and cities in Figure S1 in the supplement). Given its intensive industry and energy consumption, the city cluster was regarded as one of the largest BC emission sources in eastern China and BC emissions from this region accounted for nearly half of the total emissions in Jiangsu (Zhou et al., 2017). The heavy air pollution was found in the region: the annual averages of fine particle ($PM_{2.5}$) concentrations in all the cities exceeded the National Ambient Air Quality Standard (NAAQS, 35 μg/m^3) in 2012. Under the pressure of air quality improvement, Jiangsu conducted aggressive actions of emission control, leading to 20% reduction in the annual average of $PM_{2.5}$ concentration from 2013 to 2015. Based on a provincial bottom-up emission inventory, we estimated the contributions to BC concentrations by sector at two ground observation sites through the brute-force method in CTM. The results, together with observed ambient BC concentrations, were incorporated in a multiple regression model to derive the top-down estimate of BC emissions for southern Jiangsu city cluster. The advantage of top-down estimate against bottom-up inventory was then judged by CTM and ground observations. The factors that would potentially influence the top-down estimate were also evaluated, including number and spatial representativeness of observation sites, and initial bottom-up emission input. The uncertainties of the multiple regression model were finally evaluated including the influence of precipitation and the near-linear assumption between BC emissions and concentrations.

2 Data and method

2.1 Bottom-up inventories of BC emissions

Two bottom-up emission inventories at different spatial scales were used in this

Atmos. Chem. Phys. Discuss., https://doi.org/10.5194/acp-2018-984
Manuscript under review for journal Atmos. Chem. Phys.
Discussion started: 4 October 2018

work. At the national scale, the Multi-resolution Emission Inventory for China (MEIC, http://www.meicmodel.org/) was developed by Tsinghua University, with an original horizontal resolution at 0.25°×0.25°. At the provincial scale, Zhou et al. (2017) collected the best available information of industrial sources in Jiangsu and developed an inventory with higher resolution at 3×3 km. The latter was proved to be more supportive in air quality simulation at city cluster scale (Zhou et al., 2017; Zhao et al., 2017). In both inventories, anthropogenic BC emissions for 2012 came from four major sectors: power generation, industry, residential sources and transportation. The national and provincial inventories for 2015 (mentioned respectively as MEIC-prior and JS-prior hereinafter) were obtained using a simple scaling method based mainly on changes in activity levels (energy consumption and industrial production, etc) between the four years. Table S1 in the supplement summarizes the data sources of activity levels and the scaling factors by sector in JS-prior. As MEIC-prior includes only four major sectors, the scaling factor for each sector was calculated as the average of those for subcategories within the sector. Potential changes in BC emission factors from 2012 to 2015, e.g., those attributed to varied manufacturing technologies and/or penetrations of emission control devices, were not considered in the calculation. The implication and uncertainty from that simplified emission scaling method will be further discussed in Section 4.3. The temporal distribution of the emissions was dependent on that of activity levels by source category. Such information was investigated by Zhou et al. (2017) according to the official statistics of the country (http://data.stats.gov.cn/) and directly adopted in this work.

2.2 Top-down emission estimation with multiple regression model

The top-down emissions of BC in southern Jiangsu (mentioned as JS-posterior hereinafter) were estimated with a multiple regression model using ground observations as constraint. The regression model matched BC contributions by sector (calculated through CTM) against measured ambient hourly BC concentrations:

$$c_{obs} = \beta_1 c_{power} + \beta_2 c_{industry} + \beta_3 c_{residential} + \beta_4 c_{transportation} + \varepsilon \quad (1)$$

where c_{obs} is the vector of observed hourly BC concentrations; c_{power}, $c_{industry}$, $c_{residential}$, and $c_{transportation}$ are the vectors of BC concentrations contributed by power generation, industry, residential sources and transportation, respectively, and they were simulated using the brute-force method as described in Section 2.3; β_1-β_4 are the domain-wide scaling factors obtained by sector in the multiple regression model to best match observations; and ε is the error vector of the model.

As BC is not one of the six regulated air pollutants in the NAAQS, it was a big challenge to obtain observation data with high temporal resolution in most cities of southern Jiangsu. For the whole year 2015, hourly ambient BC concentrations were available at two sites in Nanjing, the capital of Jiangsu. As illustrated in Figure 1, one is a suburban site located in the Xianlin Campus of Nanjing University in northeast Nanjing (NJU), and the other is an urban site in Jiangsu Provincial Academy of Environmental Science (PAES). At both sites, BC was sampled and analyzed hourly with semi-continuous carbon analyzer (Model-4, Sunset Lab, USA). Details of the measurement approach were described in Chen et al. (2017). The statistics of observed ambient BC concentrations at the two sites are shown in Figure S2 in the supplement. The annual average BC concentrations (calculated as the mean of January, April, July and October) were 3.83 and 2.47 μg/m^3 at NJU and PAES, respectively. The hourly average BC observations ranged 0.06-17.65 μg/m^3 and 0.22-19.76 μg/m^3 at NJU and PAES, respectively. The values were similar to those observed in the Guanzhong basin (0.4-23.1μg/m^3), the Pearl River Delta region (1-13 μg/m^3) and the Beijing-Tianjin-Hebei region (2-32 μg/m^3) (Li et al., 2016). Much higher BC concentrations were observed in autumn and winter at both sites, with the monthly means at 3.96 and 5.44 μg/m^3 at NJU and 3.62 and 2.80 μg/m^3 at PAES, respectively.

The scaling factors derived from Eq. (1) were used to constrain BC emissions in JS-prior from a top-down perspective by assuming a near-linear relation between changes in BC concentrations and emissions:

$$E_{JS\text{-}posterior} = \beta_1 E_{power} + \beta_2 E_{industry} + \beta_3 E_{residential} + \beta_4 E_{transportation} \quad (2)$$

where $E_{JS\text{-}posterior}$ is the vector of the total BC emissions from the top-down approach; E_{power}, $E_{industry}$, $E_{residential}$ and $E_{transportation}$ are the vectors of BC emissions from power generation, industry, residential sources and transportation, respectively, in JS-prior.

2.3 Air quality simulation

We used the Models-3 Community Multi-scale Air Quality (CMAQ) version 4.7.1 to simulate ambient BC concentrations. As shown in Figure 1, three nested domains were applied with horizontal resolutions of 27, 9, and 3 km, respectively, on a Lambert Conformal Conic projection centered at (110°E, 34°N). The mother domain (D1, 177×127 cells) covered most parts of China and other surrounding countries. The second domain (D2, 118×121 cells) covered Jiangsu, Anhui, Zhejiang, Shanghai, and parts of other provinces in China . The third domain (D3, 133×73 cells) covered Shanghai, part of Anhui province and the city cluster in southern Jiangsu. There were 27 vertical levels from the ground surface up to 50 hPa on terrain-following coordinated. The simulations were conducted for January, April, July and October to represent four typical seasons in 2015. A 5-day spin-up period of each month was applied to minimize the influence of initial conditions in the simulations.

Meteorological fields were simulated by the Weather Research and Forecasting Model (WRF) version 3.4 and the carbon bond gas-phase mechanism (CB05) and AERO5 aerosol module were adopted in CMAQ. Relevant details of model configuration can be found in Zhou et al. (2017). Statistical indicators including averages of simulations and observations, bias, normalized mean bias (NMB), normalized mean error (NME), root mean squared error (RMSE) and index of agreement (IOA) were applied to evaluate the modeling performance of WRF (Baker et al, 2004; Zhang et al., 2006). Ground observation data at 1 or 3 h interval at meteorological stations including Lukou, Hongqiao and Liyang stations in the third domain (labeled in Figure 1) were taken from National Climatic Data Center (NCDC).

The statistical indicators for temperature at 2 m (T2) and relative humidity at 2 m (RH2), wind speed and direction at 10 m (WS10 and WD10) for the four typical months in 2015 are summarized in Table S2 in the supplement. Discrepancies between ground observations and WRF modeling were within acceptable range (Emery et al., 2001).

To make it applicable in our CTM, MEIC-prior was downscaled into grid systems of each modeling domain, based on the spatial distributions of gross domestic product (GDP, for power generation and industrial emissions) and population (for residential and transportation emissions) at a horizontal resolution of 1×1 km. The downscaled MEIC-prior was used for the first, the second domains and the regions outside Jiangsu of the third domains, while JS-prior was applied for the Jiangsu region of the third domain. Brute-force method was applied to estimate contributions to ambient BC concentrations by sector. Five scenarios were designed in this study: Scenario B (the base scenario) in which emissions from all sources in the third domain were included, and Scenarios S1, S2, S3, and S4 in which BC emissions from power generation, industry, residential sources and transportation were zeroed out, respectively. We compared simulated BC concentrations in S1, S2, S3 and S4 with those in Scenario B in four months, and the contributions from four major emission sectors to ambient BC levels were determined as the differences in simulated concentrations between Scenarios B and S.

3 Results

3.1 Bottom-up emission estimate

The total annual BC emissions of JS-prior were estimated at 26.99 Gg for southern Jiangsu city cluster in 2015, including 0.18 Gg from power generation, 17.67 Gg from industry, 3.80 Gg from residential sources and 5.33 Gg from transportation, as shown in Figure 2. Accounting for 66% of total annual emissions, industry was identified as the dominant contributor to BC, followed by transportation (20%) and residential sources (14%). Although the policies of energy conservation and emission control have been conducted for years, there were still a number of small facilities with low operation temperatures and combustion efficiencies in southern Jiangsu, leading to a large amount of BC from incomplete combustion. When scaling emissions from 2012 to 2015, in addition, improvements in emission controls were not taken into account, such as elevated combustion technologies and enhanced use of dust collectors. The potential reductions in net emission factors for major factories, therefore, were not well quantified, and the emissions from industry could be overestimated. Emissions from power generation were few, resulting from relatively high combustion efficiency of pulverized boilers and large penetrations and removal rates of dust collectors. Besides the annual total, the emissions of four months (January, April, July and October) were also estimated and limited seasonal differences were found as shown in Figure 2.

Figure S3 in the supplement shows the spatial distribution of annual BC emissions in JS-prior. For power generation and industry sectors, latitude and longitude of each plant were applied to allocate BC emissions, and the outstandingly high emissions shown in the map indicated the existence of big industrial plants. For residential sources, large emissions were found in the regions with intensive population. Emissions from transportation were mainly distributed along the road net and downtown regions in southern Jiangsu cities (see the geographic locations of downtowns in Figure S1 in the supplement), slightly overlapping with those from residential sources.

3.2 Top-down emission estimate

The time series of BC concentrations contributed by various sectors (*c* in Eq. (1)) were simulated with CTM and illustrated in Figures S4 and S5 in the supplement for NJU and PAES, respectively. Among all the sectors, the largest seasonal variation in BC contribution was found for residential sources. The average concentrations contributed by this sector in January reached 0.76 and 0.94 μg/m^3 at NJU and PAES, respectively, approximately double of those in another three months. The concentrations contributed by industry were significantly enhanced in certain periods (e.g., January 20th, April 9th-11th, and July 15th-17th), and industrial emissions were expected to be an important reason for the overestimation in BC concentrations through CTM (see the model evaluation in Section 3.3). Table S3 in the supplement summarizes the monthly and annual mean BC contributions by sector. The annual contributions of industry at the two sites were close to each other (21.0% and 21.9% at NJU and PAES respectively). Contributions of residential sources and transportation were higher at PAES resulting from large population and heavy traffic in the urban area. Minor contribution of power generation to BC concentrations was found at both sites (the annual means were less than 1%), attributed to its very limited emissions.

Summarized in Table 1 are the scaling factors β_1-β_4 estimated from multiple regression model (Eq. (1)) by season, together with the statistical indicators including the values of t, Sig. (or p) and variance inflation factor (VIF). The values of t and Sig. indicate statistical significance with a threshold of 2 and 0.05, respectively. VIF is a test for multicollinearity and the model is reasonable with VIF smaller than 10. Since the emissions from power generation were small and they contributed very little to ambient BC concentrations, inclusion of power generation component would not significantly improve the regression model. In this study, therefore, we assumed that the simulated BC concentrations from power generation were correct by setting β_1 at 1 and further subtracted them from the observations. Most statistical indicators in Table 1 met the criteria (t>2, Sig.<0.05, VIF<10) and the overall significance was 0.00 in four months, implying acceptable robustness of the multiple regression model. However, the results were not statistically significant indicated by t and p values for some months and sectors (e.g., industry in April and residential in April and July), implying that the constrained emissions for those month/sectors need to be cautiously analyzed.

By applying β_1-β_4 in Eq. (2), the top-down estimates of BC emissions (JS-posterior) were estimated and illustrated in Figure 2. The total BC emissions for southern Jiangsu city cluster were calculated at 13.4 Gg, 50% smaller than those of JS-prior. The scaling factors of emissions from industry and transportation (β_2 and β_4) ranged from 0.22 to 0.42 and from 0.55 to 0.79 for different months, respectively. Accordingly, the emissions from industry and transportation in JS-posterior were estimated 67% and 32% smaller than those in JS-prior, respectively. As mentioned above, the emissions in JS-prior 2015 were simply scaled from those in 2012 according to activity data, and changes in emission factors were not considered. In the actual fact, however, a series of measures in industry and transportation were conducted to improve energy efficiency and to reduce emissions over recent years. Issued in 2013, for example, the Air Pollution Control Planning for the Key Regions for the 12th Five-Year Plan period (2010-2015) aimed to achieve 7% and 15% reductions in the annual average concentration and industrial emissions of fine particles in Jiangsu province from 2010 to 2015, respectively (Qian, 2013). The measures included eliminating old and energy-inefficient plants of heavy-polluted industries (thermal power generation and steel/building material production), and optimizing the energy structure through application of sustainable energy. Meanwhile, the enhanced use of cleaner gasoline and diesel products (National stage V standard) in transportation could lead to reduced vehicle emissions. The government efforts in emissions controls proved effective, indicated by the scaling factors much smaller than 1 (β_2 and β_4 in Table 1) and the reduced emissions of JS-posterior. For residential sources, the emissions in JS-posterior were 3% smaller than those in JS-prior, indicating limited difference in the annual total emissions between the two inventories. However, the scaling factors (β_3) in January and October were 1.31 and 1.52 respectively, showing a stronger enhancement in BC emissions in winter and autumn in JS-posterior than those in JS-prior. It thus implied that there were missing sources likely associated with low-quality fossil fuels or biofuel used for heating in winter and crop waste burning in autumn in JS-prior. For the capital city of Jiangsu Province, Nanjing, Huang et al. (in preparation) conducted detailed analysis on the changes in operation activities and emission control technologies of individual sources based on annually updated official environmental statistics and pollution census. With the bottom-up approach, the annual BC emissions in the city were estimated to decrease by 60% from 2012 to 2015 as shown in Figure S6 in the supplement. The relative change in annual emissions was close to that between JS-prior and JS-posterior, and the validity of the two methods (the bottom-up approach by Huang et al. and the top-down approach in this work) could be verified.

Figure 3 presents the seasonal variations in BC emissions of JS-prior, JS-posterior and MEIC-prior by sector, and stronger variations were generally found in JS-posterior. As shown in Figure 3a, the largest difference among the three inventories existed in the residential sources, and the ratio of maximum to minimum monthly emissions was 4.33 in JS-posterior, close to that in MEIC-prior at 4.00 and nearly 4 times of that in JS-prior at 1.13. The analogue ratio for industry was 2.05 in JS-posterior, nearly twice of those in JS-prior at 1.14 and MEIC-prior at 1.12. The smallest difference was found for transportation among the three inventories. Seasonal variations in total emissions were a combination of those by sector weighted by the contribution of each sector to total emissions. The ratios of maximum to minimum monthly emissions were 1.13, 1.83 and 1.29 for JS-prior, JS-posterior and MEIC-prior, respectively (Figure 3b). The value for JS-posterior was closer to 2.1 for an anthropogenic BC emission inventory in China by Lu et al. (2011) that considered enhanced use of fossil fuels for residential heating in winter in northern China. The comparison thus implied again that current bottom-up inventories might underestimate the emissions of residential solid fuel burning in winter in southern Jiangsu. As central household heating was not conducted in the area in winter, the official energy statistics on which bottom-up inventories were based may not fully capture the elevated fuel burning by disperse households. Spatial distribution of BC emissions in JS-posterior was illustrated in Figure S3 in the supplement. Compared to JS-prior, BC emissions from industry and transportation were greatly reduced in downtown regions in southern Jiangsu city cluster.

3.3 Evaluation of the top-down emission estimate

The simulated BC concentrations based on bottom-up (JS-prior) and top-down estimation in emissions (JS-posterior) were compared with observations to evaluate the two inventories, and the results were illustrated in Figures 4 and 5 for NJU and PAES sites, respectively. Statistical indicators including mean concentrations from simulations and observations, NMB and NME, as well as the regression correlation (R) were calculated to evaluate the modeling performance, as summarized in Table 2.

In general, CTM based on JS-prior reproduced well the temporal variations of the observed BC concentrations at the two sites. The highest and lowest concentrations were respectively simulated in winter and summer, consistent with observations with an exception at PAES where the observed monthly mean in January (2.80 μg/m^3) was lower than that in October (3.62 μg/m^3). The seasonal variation of BC concentrations at NJU was larger than that at PAES, suggesting bigger impact of household solid fuel use on the suburban and rural regions. Though the model was able to capture the seasonal variability, discrepancies between simulations and observations existed, and CTM commonly underestimated BC concentrations at the suburban site NJU and overestimated those at the urban site PAES. With the monthly means ranged 1.99-5.97 μg/m^3 at NJU, the annual average of BC concentration (calculated as the mean of January, April, July and October) was simulated at 3.44 μg/m^3, smaller than the observed 3.83 μg/m^3. With the monthly means ranged 2.61-6.46 μg/m^3, in contrast, the annual concentration at PAES was simulated at 3.39 μg/m^3, larger than the observed 2.48 μg/m^3. Better correlation between observation and simulation was found at NJU, indicated by the larger R. The annual mean NMBs were calculated at -10.16% and 36.67%, and the NMEs were 41.15% and 72.00% at NJU and PAES, respectively. The discrepancy suggested that JS-prior used in CTM might misrepresent the spatial pattern of emissions. Population and economy densities were applied to allocate BC emissions, leading to overestimation in emissions and thereby simulated concentrations in urban areas with more population and economic activity. Besides, the model overestimated the peak surface concentrations at both sites particularly when the contribution from industry sector was enhanced as mentioned in Section 3.2 (e.g., January 9th-11th and April 9th-10th at NJU, and April 9th-12th, the second half of July, and October 20th at PAES).

Application of JS-posterior in CTM effectively corrected large biases between simulations and observations at the two sites. As shown in Table 2, NMEs were reduced for most months while effects of applying JS-posterior in CTM varied at two sites. At PAES, the annual average NME declined from 72.00% to 57.55% and the annual mean of BC concentration was simulated at 2.57 μg/m^3, in better agreement with the observed 2.48 μg/m^3 than the simulated 3.39 μg/m^3 using JS-prior. The largest reductions in NMEs were found in April and July, from 73.18% to 42.87% and from 92.74% to 42.37%, respectively. Moreover the overestimation in peak concentrations using JS-prior were partly corrected when JS-posterior was applied, resulting mainly from the reduced emissions from industry and transportation. Although simulation of peak concentrations at NJU were improved as well, the annual average NME at NJU slightly increased from 41.15% to 44.16% and the annual mean of BC concentration was simulated at 2.82 μg/m^3, smaller than the simulated 3.44 μg/m^3 using JS-prior. Bigger bias was found in July and October at NJU, since the reduced emission estimates in JS-posterior led to further underestimation in simulated ambient BC levels compared to JS-prior. Limitation of current multiple regression model was thus indicated that overestimation and underestimation in concentrations at different sites could hardly be corrected simultaneously without further improvement in spatial distribution of emissions.

4 Discussions

We selected April to evaluate the sensitivity of observation and bottom-up emission input to top-down constraint. Observation site number, spatial representativeness of sites, and initial bottom-up inventory were changed separately in the constraining approach, and various top-down estimates could be derived and compared with each other. The statistical indicators of modeling performances based on different bottom-up and top-down emission estimates in April are summarized in Table 3. Furthermore, we evaluated the uncertainty of the multiple regression model, including the assumption of near linearity between emissions and concentrations and the impact of precipitation. Details were described as below.

4.1 The effect of observation site number

A major challenge in understanding the sources and distributions of BC in China was lack of a consistent and stable measurement network with good spatiotemporal coverage, such as the IMPROVE network in the United States (Malm et al., 1994). Uncertainty existed in the top-down estimates in this work, as hourly measurements on BC concentrations were only available at two sites in southern Jiangsu. Therefore, besides JS-posterior derived from observations at both sites as described in Section 3.2 (mentioned as Case 1 hereinafter), we conducted a Case 2 in which observation data at only one site (NJU) was used in the top-down approach, to analyze the effect of the site number on emission estimates. The scaling factors of emissions from industry, residential sources and transportation were recalculated at 0.42, 0.95 and 0.65, respectively. Compared with Scenario B, the NMEs of Case 2 decreased from 42.31% to 32.47% and from 73.18% to 61.59% at NJU and PAES, respectively, implying the benefits of ground measurements (even available only at one site) on emission constraint. The NME in Case 2 was slightly smaller than that in Case 1 at NJU, suggesting that application of measurement data at one single site could improve model performance moderately at that site. At PAES, in contrast, much larger

Atmos. Chem. Phys. Discuss., https://doi.org/10.5194/acp-2018-984
Manuscript under review for journal Atmos. Chem. Phys.
Discussion started: 4 October 2018

NME was found in Case 2. Much better model performance in Case 1 at PAES indicated that inclusion of more measurements with better spatiotemporal coverage could constrain BC emissions at city cluster level more effectively.

4.2 The effect of spatial representativeness of observation sites

Spatial representativeness of observation sites was identified and its impact on top-down emission constraint was evaluated. Considering the prevailing winds from northeast and southeast, on one hand, NJU located upwind Nanjing is hardly influenced by the emissions from the downtown of the city. Besides the site is downwind of the Yangtze River Delta region (YRD) including the Suzhou–Wuxi–Changzhou-Zhenjiang city cluster (Chen et al., 2017), thus it is more representative for the western YRD emissions through regional transport. On the other hand, PAES is located at urban Nanjing and its air quality is commonly influenced by surrounding transportation, residential, and commercial sources, thus the site is representative for the local emissions of Nanjing. In contrast to previous top-down studies that did not distinguish influence of local emissions and transport on air quality in sub-regions of the research domain (Wang et al., 2011; Fu et al., 2012), the spatial representativeness of the two observation sites were taken into account to improve the top-down approach and the result of constraining BC emissions in southern Jiangsu city cluster. Through the brute-force method described in Section 2.3, we zeroed out the emissions from Nanjing and Suzhou–Wuxi–Changzhou-Zhenjiang city cluster in CTM, respectively, and compared the simulated concentrations with those in Scenario B to analyze the contributions of the two regions to ambient BC concentrations at NJU and PAES sites. As shown in Figure S7 in the supplement, the contribution of emissions from Nanjing to PAES was greater than that to NJU in 82% of the modeling period, and the analogue number was 81% for the contribution of Suzhou–Wuxi–Changzhou-Zhenjiang city cluster to NJU greater than that to PAES. We thus concluded that emissions from Nanjing contributed significantly to PAES while those from Suzhou–Wuxi–Changzhou-Zhenjiang city cluster contributed significantly to NJU. We then developed a new case of top-down emission estimate in southern Jiangsu (Case 3), in which observation data at PAES and NJU were applied to constrain emissions from Nanjing and Suzhou–Wuxi–Changzhou-Zhenjiang city cluster, respectively.

The scaling factors in Case 3 are provided in Table 4. To avoid the collinearity in the multiple regression model, we expected that the relative changes in emissions from transportation in Nanjing and Suzhou–Wuxi–Changzhou-Zhenjiang city cluster were similar for recent years, resulting from the same progress of emission standard implementation (National Standard Stage IV) in southern Jiangsu and the frequent circulation of vehicles among the cities. Therefore a same scaling factor was assumed for transportation in the two regions. As shown in Table 4, all the scaling factors at PAES were smaller than those at NJU, implying that implementation of emission controls in Nanjing were more stringent than that in Suzhou–Wuxi–Changzhou-Zhenjiang city cluster from 2012 to 2015. As the host city of the 2nd Asian Youth Games in 2013 and the 2nd Youth Olympic Games in 2014, Nanjing was undertaking series of restrictions on air pollutant emissions. The city conducted emission control action on small coal-fired boilers since 2013 and over 1200 coal-fired boilers had been shut down by the end of 2014. In addition, central heating units were largely applied to replace the coal with electricity, natural gas or biofuel. As shown in Table 3, the NMEs in Case 3 were the smallest at both sites among all the cases with an exception: the NME at NJU in Case 3 was 32.64%, slightly larger than that in Case 2 at 32.47%. The result implied that inclusion of more measurement data with their spatial representativeness considered could improve the top-down approach in terms of spatial distribution of emissions and could reduce the deviation between observations and simulations.

Summarized in Table 5 are BC emissions from Nanjing and Suzhou–Wuxi–Changzhou-Zhenjiang city cluster estimated in different cases. All the top-down estimates were approximately half of the bottom-up estimate and the estimate in Case 1 was the smallest among all the cases. The same scaling factors were generated and applied in Cases 2 and 3 to calculate BC emissions from Suzhou–Wuxi–Changzhou-Zhenjiang city cluster which accounted for 80% of the total emissions in southern Jiangsu, resulting in similar top-down emission estimates between the two cases.

4.3 The effect of initial bottom-up emission input

Given the large uncertainty in JS-prior that was simply developed based on the changes of activity levels in recent years, we applied MEIC-prior as well to explore the effect of initial emission inventory on top-down BC constraints.

Figures 6 and 7a compare the total amount and spatial distribution of emissions between JS-prior and MEIC-prior in April, respectively. The total BC emissions of southern Jiangsu city cluster in JS-prior were 21% lower than those in MEIC-prior. In JS-prior, as shown in Figure 7a, the emissions from some industrial plants were extremely larger than those in MEIC-prior, while the emissions in urban areas were found smaller. Both inventories indicated extremely small contribution from power generation. BC emissions from industry sector were calculated at 1.34 Gg in JS-prior, 0.22 Gg smaller than MEIC-prior. Emissions from industry in MEIC-prior were calculated based on regional average of emission factors and allocated according to spatial distribution of GDP. The method would possibly result in underestimation in emissions from big industrial plants but overestimation in urban areas. Emissions from residential sources in JS-prior were close to those in MEIC-prior as similar methodology was applied for the sector in the two inventories. BC emissions from transportation in MEIC-prior (0.85 Gg) were twice of those in JS-prior (0.42 Gg) attributable probably to the application of different emission factors. For on-road transportation, the emission factors in JS-prior were calculated with CORPERT model (EEA, 2012; Zhou et al., 2017) while they were obtained from available domestic measurements in MEIC-prior.

Simulation Case 4 was determined using MEIC-prior in CTM. As shown in

Table 3, the hourly average of BC concentrations at NJU was simulated at 2.49 μg/m^3 for April 2015 in Case 4, close to 2.38 μg/m^3 simulated with JS-prior (Scenario B). At PAES, however, application of MEIC-prior in CTM resulted in much larger concentration than JS-prior (5.13 versus 2.98 μg/m^3), indicating again that MEIC-prior would overestimate the emissions in urban area. Following the top-down approach described in Section 2.2, we developed Case 5, using MEIC-prior instead of JS-prior as the initial input of emission data in CTM. The scaling factors of emissions from industry, residential sources and transportation were respectively calculated at 0.15, 1.30 and 0.25 through multiple regression model, and the top-down estimate in BC emissions (mentioned as MEIC-posterior hereafter) were calculated at 0.75 Gg in April 2015, close to 0.78 Gg in the JS-posterior (Figure 6). The differences in the emissions from industry and transportation between JS-posterior and MEIC-posterior were 0.06 and 0.07 Gg, respectively, much smaller than those between JS-prior and MEIC-prior. Besides the total amount, differences in spatial distribution in industry plants and urban area between the top-down estimates (JS-posterior and MEIC-posterior) were also significantly reduced compared to those between bottom-up estimates (JS-prior and MEIC-prior), as shown in Figure 7b. Figure 8 illustrates the scatterplots of the simulated BC concentrations from bottom-up and top-down inventories at NJU (Figure 8a) and PAES (Figure 8b). Using two bottom-up inventories in CTM, bigger difference in simulated BC concentrations was found at PAES compared to that at NJU, indicated by the slope (1.10) closer to 1 at NJU in Figure 8a. The correlation coefficients (R^2) between simulated BC concentrations using JS-prior and MEIC-prior were 0.81 at NJU and 0.40 at PAES respectively. Using two top-down estimates, the difference between simulated concentrations at PAES was significantly reduced and the slope got much closer to 1 in Figure 8b. The correlation coefficients (R^2) were enhanced to 0.94 and 0.87 at NJU and PAES, respectively. To summarize, similar results from top-down constraint approach could be obtained in emission level, spatial distribution, and CTM performance, even clear difference existed in the initial bottom-up inventories. In other word, limited effect of initial emission input was evaluated on the top-down estimate from the multiple regression model.

4.4 Uncertainty analysis of the multiple regression model

As mentioned in Section 2.2, the assumption of near linearity between emissions and concentrations is a principle of the multiple regression model, given the weak chemistry reactivity of BC. The principle has been applied in previous studies to constrain BC emissions (Fu et al., 2012; Kondo et al., 2011; Wang et al., 2013; Park et al., 2003; Verma et al., 2017). In the actual fact, however, processes other than chemical reaction, e.g., precipitation or wet deposition, impact the linearity. Therefore, the near-linear assumption needs to be justified, and the uncertainty of the methodology could then be evaluated.

Sensitivity analysis was conducted to assess the rationality of brute-force method described in Section 2.3, in which emissions of given sector were zeroed out to determine their contribution to the ambient concentrations. As summarized in Table S4 in the supplement, we first calculated the ratio of simulated wet deposition to emissions by month for NJU, PAES and the whole southern Jiangsu city cluster with JS-prior (Scenario B) and JS-posterior (Case 1), respectively. July and October were identified as the months with the most and least impact from precipitation, suggested by the largest and smallest ratio, respectively. Two sensitivity simulations were then conducted for the selected two months, in which doubled and halved emissions (i.e., 200% and 50% of emissions in JS-prior, respectively) were used in CTM, and the simulated concentrations were then compared to those with JS-prior (i.e., Scenario B). Figures 9 and 10 illustrate the linear correlations of the simulated concentrations in these two sensitivity cases and the base scenario (Scenario B) at NJU and PAES, respectively. As can be seen in all the panels, the fraction of change in simulated monthly average concentration ($F_{conc.}$) was close to that of emission change ($F_{emis.}$), i.e., the ratio of $F_{emis.}$ to $F_{conc.}$ was around 1.0, within a range of ±10%. Similar ratio of

Atmos. Chem. Phys. Discuss., https://doi.org/10.5194/acp-2018-984
Manuscript under review for journal Atmos. Chem. Phys.
Discussion started: 4 October 2018

Atmospheric Chemistry and Physics Discussions

change in emissions ($\triangle E$) to that in simulated average concentration ($\triangle C$) was obtained for each month and site as well. The results thus suggested that the impact of non-linearity between emissions and concentrations was limited, no matter the precipitation was strong or not. As the top-down constrained emissions (JS-posterior) were 50% smaller than the bottom-up estimates (JS-prior), the relative change was far beyond the uncertainty from non-linearity (±10%), implying the improvement of the top-down approach on emission estimation.

Many studies have reported the difficulty in precipitation simulation with WRF (Annor et al., 2017; Liu et al., 2018; Yu et al., 2011; Yang et al., 2014; Kaewmesri, 2018). In this study, the observed ground precipitation at Lukou, Liyang and Shanghai stations (see Figure 1 for locations) was compared with the simulated one to evaluate the WRF performance for precipitation modeling. As shown in Figures S8-11 in the supplement, the model could capture the dates of precipitation, but it generally overestimated the amount. Similar results were found in previous studies that WRF overestimated precipitation at fine spatial resolution (Politi et al., 2018; Kotlarski et al., 2014; García-Díez et al., 2015). Improvement in physics parameterization schemes in WRF will help better understanding the wet deposition of BC through simulation. To further evaluate the effect of wet deposition on emission constraining, we conducted an extra Case 6, in which the data influenced by simulated wet deposition (i.e., the periods with simulated wet deposition at hourly basis) were excluded in the top-down approach. The new scaling factors β_1'-β_4' estimated from the multiple regression model were summarized in Table 6. By applying β_1'-β_4' in Eq. (2), the top-down estimates of BC emissions in Case 6 were calculated at 13.7 Gg, and the emissions by sector and month were illustrated in Table 7, together with the relative deviation (RD) compared to emissions in Case 1(JS-posterior). The relative deviations of monthly total emissions between Case 6 and Case 1 were less than 5%, with an exception of July at 14%, and that for annual total was 2.6%. Larger relative deviations were found for given sources, e.g., residential in January and transportation

Atmos. Chem. Phys. Discuss., https://doi.org/10.5194/acp-2018-984
Manuscript under review for journal Atmos. Chem. Phys.
Discussion started: 4 October 2018

Atmospheric Chemistry and Physics Discussions

in July. The deviations, therefore, were much smaller than that between the emissions in JS-prior and JS-posterior. We consequently applied CTM to evaluate the model performance with the emissions in Case 6 for July. Illustrated in Table 8 were the simulated BC concentrations and the statistic indicators obtained through comparisons with observation at the two sites. As suggested by the NME and R values, little improvement on CTM performance was achieved with the emissions in Case 6, compared to those with Case 1 (Table 2). The impact of simulated wet deposition on the top-down approach was thus expected to be moderate in this work.

As the simulated wet deposition varied from the reality to some extent and the impact of precipitation along the transport was not excluded in Case 6, we selected July to conduct a Case 7, in which the data influenced by accumulative precipitation along the back trajectories at the two sites were excluded in the multiple regression model. The merged high-quality precipitation measured by the Tropical Rainfall Measuring Mission (TRMM) satellite instrument was adopted for wet deposition screening, with a temporal resolution of 3 h and a spatial resolution of 0.25°×0.25°. We used the Hybrid Single Particle Lagrangian Integrated Trajectory (HYSPLIT, version 4.9) model (http://www.ready.noaa.gov) to calculate the 48 h back trajectories of the air masses arriving at NJU and PAES. The back trajectories were calculated every 3 hour for July with the simulated layer heights of 50, 100 and 500 m above the ground and the time step of 3 h (the same as the temporal resolution of TRMM). The hourly accumulative precipitation along the 48 h back trajectories at two sites were then calculated to determine the BC-CO data pairs influenced by precipitation, given the little effect of precipitation on CO. Figure 11 illustrates the changes in the ⊿BC/⊿CO ratio observed at two sites for different accumulated precipitation intervals. At NJU, the ⊿BC/⊿CO ratio of air masses receiving less than 3 mm accumulated precipitation was significantly larger than that of air masses receiving more than 3 mm, and the analogue number was 5 mm at PAES. In Case 7, therefore, we excluded the BC-CO data pairs receiving more than 3 mm and 5 mm accumulated precipitation along their trajectories within the last 48 h at NJU and PAES, respectively, in the multiple regression model. It minimized the effect of wet deposition while retained sufficient data points for the statistical significance. Figure 12 shows the simulated wet deposition in Case 6 and the accumulated precipitation in Case 7 for July to compare the data selection in the two cases. In Case 6, the number of data points were reduced to 65% of Case 1 after data screening, and over 500 samples at the two sites were available for the multiple regression model. In Case 7, only 31% of data points remained. The periods excluded in Case 7 contained those in Case 6, implying a stricter data screening to eliminate the effect of precipitation.

Table 9 shows the scaling factors estimated from the multiple regression model in Case 7, and no big changes were found compared to the scaling factors for July in Case 6 (Table 6). Consequently, the emissions by sector and total emissions in Case 7 were close to those in Case 6 (Table 7). The relative deviation of total emissions in July between Case 7 and Case 1 (RD in Table 9) was 13%, and those for residential and transportation were larger. The influence of precipitation was again indicated insignificant, as the deviation was much smaller than that between the estimates obtained from the bottom-up and top-down methods. Moreover, the CTM performance based on Case 7, indicated by NMB and NME, was found similar to that based on Case 6, implying the small effect of precipitation screening on simulation. Even excluding the influence of precipitation along the back trajectories, the Sig. for residential sources in Case 7 was still much larger than 0.05 (Table 9), suggesting more efforts on quantification of emissions for this highly uncertain source category.

5 Conclusions

Monthly top-down estimates of BC emissions were derived from a multiple regression model that integrated CTM and hourly BC concentrations from two ground observation sites in southern Jiangsu city cluster. The annual emissions from top-down approach (JS-posterior) were estimated at 13.4 Gg for 2015, 50.3% smaller than those in bottom-up emission inventory that did not include the improved emission controls in recent years (JS-prior), implying the effectiveness of air pollution prevention measures on emission abatement. Application of JS-posterior in CTM reduced the deviations between simulations and observations at two ground sites effectively, especially at the urban site PAES. To evaluate the effects of observation data on top-down estimate, two more cases in which observation data of only one site (NJU) and observation data at both sites with their spatial representativeness differentiated were applied to constrain the emissions, respectively. Best CTM performance was found for the third case, indicating that inclusion of more ground measurements with better spatiotemporal coverage in the city cluster would improve the understanding of spatial distributions of BC emissions. In addition, top-down estimates were derived from various bottom-up inventories, and the differences in emission amount, spatial distribution and CTM performance between the constrained emission estimates were significantly reduced compared to those between the bottom-up inventories. The results implied that changes in initial emission input in the regression model and CTM had limited effect on the top-down estimation. Finally, the assumption of near-linearity between emissions and concentrations was justified, and the influence of wet deposition on the estimated emissions was evaluated to be moderate. This work demonstrated that top-down approach based on ground observations and CTM could capture the fast changes in BC emissions attributed to tightened pollution control policy at a city cluster scale. To further reduce uncertainty of the approach, more ground measurements with sufficient temporal resolution would be recommended at other regions in the city cluster. Data from other sources, such as aerosol optical depth from satellite observation, could also be included to improve the spatial and temporal distributions of emission estimates.

Acknowledgement

This work was sponsored by the National Key Research and Development Program of China (2017YFC0210106 and 2016YFC0201507), Natural Science

Foundation of China (91644220 and 41575142). We would like to acknowledge Tong Dan from Tsinghua University for national emission data (MEIC).

References

Annor, T., Lamptey, B., Wagner, S., Oguntunde, P., Arnault, J., Heinzeller, D., and Kunstmann, H.: High-resolution long-term WRF climate simulations over Volta Basin. Part 1: validation analysis for temperature and precipitation, Theoretical and Applied Climatology, 133, 829-849, 10.1007/s00704-017-2223-5, 2017.

Baker, K., Johnson, M., and King, S.: Meteorological modeling performance summary for application to $PM_{2.5}$/haze/ozone modeling projects, Lake Michigan Air Directors Consortium, Midwest Regional Planning Organization, Des Plaines, Illinois, USA, 57 pp., 2004.

Bond, T. C., Streets, D. G., Yarber, K. F., Nelson, S. M., Woo, J. H., and Klimont, Z.: A technology-based global inventory of black and organic carbon emissions from combustion, Journal of Geophysical Research-Atmospheres, 109, 10.1029/2003jd003697, 2004.

Bond, T. C., Doherty, S. J., Fahey, D. W., Forster, P. M., Berntsen, T., DeAngelo, B. J., Flanner, M. G., Ghan, S., Kaercher, B., Koch, D., Kinne, S., Kondo, Y., Quinn, P. K., Sarofim, M. C., Schultz, M. G., Schulz, M., Venkataraman, C., Zhang, H., Zhang, S., Bellouin, N., Guttikunda, S. K., Hopke, P. K., Jacobson, M. Z., Kaiser, J. W., Klimont, Z., Lohmann, U., Schwarz, J. P., Shindell, D., Storelvmo, T., Warren, S. G., and Zender, C. S.: Bounding the role of black carbon in the climate system: A scientific assessment, Journal of Geophysical Research-Atmospheres, 118, 5380-5552, 10.1002/jgrd.50171, 2013.

Cao, G., Zhang, X., and Zheng, F.: Inventory of black carbon and organic carbon emissions from China, Atmospheric Environment, 40, 6516-6527, 10.1016/j.atmosenv.2006.05.070, 2006.

Chen, D., Cui, H., Zhao, Y., Yin, L., Lu, Y., and Wang, Q.: A two-year study of

Atmos. Chem. Phys. Discuss., https://doi.org/10.5194/acp-2018-984
Manuscript under review for journal Atmos. Chem. Phys.
Discussion started: 4 October 2018

carbonaceous aerosols in ambient PM2.5 at a regional background site for western Yangtze River Delta, China, Atmospheric Research, 183, 351-361, 10.1016/j.atmosres.2016.09.004, 2017.

Cohen, J. B., and Wang, C.: Estimating global black carbon emissions using a top-down Kalman Filter approach, Journal of Geophysical Research: Atmospheres, 119, 307-323, 10.1002/2013jd019912, 2014.

Dachs, J., and Eisenreich, S. J.: Adsorption onto aerosol soot carbon dominates gas-particle partitioning of polycyclic aromatic hydrocarbons, Environmental science & technology, 34, 3690-3697, 10.1021/es991201+, 2000.

EEA (European Environment Agency): COPERT 4-Computer Programme to Calculate Emissions from Road Transport, User Manual (Version 9.0), Copenhagen, Denmark, 2012.

Emery, C., Tai, E., and Yarwood, G.: Enhanced meteorological modeling and performance evaluation for two Texas ozone episodes, 2001.

Fu, T. M., Cao, J. J., Zhang, X. Y., Lee, S. C., Zhang, Q., Han, Y. M., Qu, W. J., Han, Z., Zhang, R., Wang, Y. X., Chen, D., and Henze, D. K.: Carbonaceous aerosols in China: top-down constraints on primary sources and estimation of secondary contribution, Atmospheric Chemistry and Physics, 12, 2725-2746, 10.5194/acp-12-2725-2012, 2012.

García-Díez, M., Fernández, J., and Vautard, R.: An RCM multi-physics ensemble over Europe: multi-variable evaluation to avoid error compensation, Clim. Dyn., 45, 3141-3156, 10.1007/s00382-015-2529-x, 2015.

Gilardoni, S., Vignati, E., and Wilson, J.: Using measurements for evaluation of black carbon modeling, Atmospheric Chemistry and Physics, 11, 439-455, 10.5194/acp-11-439-2011, 2011.

Guerrette, J. J., and Henze, D. K.: Four-dimensional variational inversion of black carbon emissions during ARCTAS-CARB with WRFDA-Chem, Atmospheric Chemistry and Physics, 17, 7605-7633, 10.5194/acp-17-7605-2017, 2017.

Atmos. Chem. Phys. Discuss., https://doi.org/10.5194/acp-2018-984
Manuscript under review for journal Atmos. Chem. Phys.
Discussion started: 4 October 2018

Atmospheric Chemistry and Physics Discussions

Hong, C., Zhang, Q., He, K., Guan, D., Li, M., Liu, F., and Zheng, B.: Variations of China's emission estimates: response to uncertainties in energy statistics, Atmospheric Chemistry and Physics, 17, 1227-1239, 10.5194/acp-17-1227-2017, 2017.

Hu, Z., Zhao, C., Huang, J., Leung, L. R., Qian, Y., Yu, H., Huang, L., and Kalashnikova, O. V.: Trans-Pacific transport and evolution of aerosols: evaluation of quasi-global WRF-Chem simulation with multiple observations, Geoscientific Model Development, 9, 1725-1746, 10.5194/gmd-9-1725-2016, 2016.

Huang, Y., Zhao, Y, Qiu, L., Xie, F., Zhang, J., Huang, X.: The impacts of emission control and meteorology variation on reduced ambient $PM_{2.5}$ concentrations for a typical industrial city in Yangtze River Delta, China (in preparation).

Jacobson, M. Z.: Strong radiative heating due to the mixing state of black carbon in atmospheric aerosols, Nature, 409, 695-697, 10.1038/35055518, 2001.

Kaewmesri, P.: The Performance of Microphysics Scheme in Wrf Model for Simulating Extreme Rainfall Events, International Journal of GEOMATE, 15, 10.21660/2018.51.59256, 2018.

Koch, D., Schulz, M., Kinne, S., McNaughton, C., Spackman, J. R., Balkanski, Y., Bauer, S., Berntsen, T., Bond, T. C., Boucher, O., Chin, M., Clarke, A., De Luca, N., Dentener, F., Diehl, T., Dubovik, O., Easter, R., Fahey, D. W., Feichter, J., Fillmore, D., Freitag, S., Ghan, S., Ginoux, P., Gong, S., Horowitz, L., Iversen, T., Kirkevag, A., Klimont, Z., Kondo, Y., Krol, M., Liu, X., Miller, R., Montanaro, V., Moteki, N., Myhre, G., Penner, J. E., Perlwitz, J., Pitari, G., Reddy, S., Sahu, L., Sakamoto, H., Schuster, G., Schwarz, J. P., Seland, O., Stier, P., Takegawa, N., Takemura, T., Textor, C., van Aardenne, J. A., and Zhao, Y.: Evaluation of black carbon estimations in global aerosol models, Atmospheric Chemistry and Physics, 9, 9001-9026, 10.5194/acp-9-9001-2009, 2009.

Kondo, Y., Oshima, N., Kajino, M., Mikami, R., Moteki, N., Takegawa, N., Verma, R. L., Kajii, Y., Kato, S., and Takami, A.: Emissions of black carbon in East Asia estimated from observations at a remote site in the East China Sea, Journal of Geophysical Research-Atmospheres, 116, 10.1029/2011jd015637, 2011.

Kotlarski, S., Keuler, K., Christensen, O. B., Colette, A., Déqué, M., Gobiet, A., Goergen, K., Jacob, D., Lüthi, D., van Meijgaard, E., Nikulin, G., Schär, C., Teichmann, C., Vautard, R., Warrach-Sagi, K., and Wulfmeyer, V.: Regional climate modeling on European scales: a joint standard evaluation of the EURO-CORDEX RCM ensemble, Geoscientific Model Development, 7, 1297-1333, 10.5194/gmd-7-1297-2014, 2014.

Kurokawa, J., Ohara, T., Morikawa, T., Hanayama, S., Janssens-Maenhout, G., Fukui, T., Kawashima, K., and Akimoto, H.: Emissions of air pollutants and greenhouse gases over Asian regions during 2000-2008: Regional Emission inventory in ASia (REAS) version 2, Atmospheric Chemistry and Physics, 13, 11019-11058, 10.5194/acp-13-11019-2013, 2013.

Lei, Y., Zhang, Q., He, K. B., and Streets, D. G.: Primary anthropogenic aerosol emission trends for China, 1990-2005, Atmospheric Chemistry and Physics, 11, 931-954, 10.5194/acp-11-931-2011, 2011.

Li, N., Fu, T. M., Cao, J. J., Zheng, J. Y., He, Q. Y., Long, X., Zhao, Z. Z., Cao, N. Y., Fu, J. S., and Lam, Y. F.: Observationally-constrained carbonaceous aerosol source estimates for the Pearl River Delta area of China, Atmospheric Chemistry and Physics Discussions, 15, 33583-33629, 10.5194/acpd-15-33583-2015, 2015.

Li, N., He, Q., Tie, X., Cao, J., Liu, S., Wang, Q., Li, G., Huang, R., and Zhang, Q.: Quantifying sources of elemental carbon over the Guanzhong Basin of China: A consistent network of measurements and WRF-Chem modeling, Environmental pollution, 214, 86-93, 10.1016/j.envpol.2016.03.046, 2016.

Liu, D., Yang, B., Zhang, Y., Qian, Y., Huang, A., Zhou, Y., and Zhang, L.: Combined impacts of convection and microphysics parameterizations on the simulations of precipitation and cloud properties over Asia, Atmospheric Research, 212, 172-185, 10.1016/j.atmosres.2018.05.017, 2018.

Lu, Z., Zhang, Q., and Streets, D. G.: Sulfur dioxide and primary carbonaceous aerosol emissions in China and India, 1996-2010, Atmospheric Chemistry and Physics, 11, 9839-9864, 10.5194/acp-11-9839-2011, 2011.

Malm, W. C., Sisler, J. F., Huffman, D., Eldred, R. A., and Cahill, T. A.:Spatial and seasonal trends in particle concentration and optical extinction in the United States , Journal of Geophysical Research-Atmospheres, 99, 1347-1370, 10.1029/93jd02916, 1994.

Matsui, H., Koike, M., Kondo, Y., Oshima, N., Moteki, N., Kanaya, Y., Takami, A., and Irwin, M.: Seasonal variations of Asian black carbon outflow to the Pacific: Contribution from anthropogenic sources in China and biomass burning sources in Siberia and Southeast Asia, Journal of Geophysical Research-Atmospheres, 118, 9948-9967, 10.1002/jgrd.50702, 2013.

Ohara, T., Akimoto, H., Kurokawa, J., Horii, N., Yamaji, K., Yan, X., and Hayasaka, T.: An Asian emission inventory of anthropogenic emission sources for the period 1980-2020, Atmospheric Chemistry and Physics, 7, 4419-4444, 10.5194/acp-7-4419-2007, 2007.

Park, R. J.: Sources of carbonaceous aerosols over the United States and implications for natural visibility, Journal of Geophysical Research, 108, 10.1029/2002jd003190, 2003.

Politi, N., Nastos, P. T., Sfetsos, A., Vlachogiannis, D., and Dalezios, N. R.: Evaluation of the AWR-WRF model configuration at high resolution over the domain of Greece, Atmospheric Research, 208, 229-245, 10.1016/j.atmosres.2017.10.019, 2018.

Qian, W.: Air Pollution Control Planning for the Key Regions during the 12th Five-Year Plan period (2010-2015), China Environmental Protection Industry, 4-18, 2013.

Qin, Y., and Xie, S. D.: Spatial and temporal variation of anthropogenic black carbon emissions in China for the period 1980-2009, Atmospheric Chemistry and Physics, 12, 4825-4841, 10.5194/acp-12-4825-2012, 2012.

Ramanathan, V., and Carmichael, G.: Global and regional climate changes due to black carbon, Nature Geoscience, 1, 221-227, 10.1038/ngeo156, 2008.

Streets, D. G., Gupta, S., Waldhoff, S. T., Wang, M. Q., Bond, T. C., and Bo, Y. Y.: Black carbon emissions in China, Atmospheric Environment, 35, 4281-4296, 10.1016/s1352-2310(01)00179-0, 2001.

Streets, D. G., Bond, T. C., Carmichael, G. R., Fernandes, S. D., Fu, Q., He, D., Klimont, Z., Nelson, S. M., Tsai, N. Y., Wang, M. Q., Woo, J. H., and Yarber, K. F.: An inventory of gaseous and primary aerosol emissions in Asia in the year 2000, Journal of Geophysical Research-Atmospheres, 108, 10.1029/2002jd003093, 2003.

Verma, S., Reddy, D. M., Ghosh, S., Kumar, D. B., and Chowdhury, A. K.: Estimates of spatially and temporally resolved constrained black carbon emission over the Indian region using a strategic integrated modelling approach, Atmospheric Research, 195, 9-19, 10.1016/j.atmosres.2017.05.007, 2017.

Wang, Y., Wang, X., Kondo, Y., Kajino, M., Munger, J. W., and Hao, J.: Black carbon and its correlation with trace gases at a rural site in Beijing: Top-down constraints from ambient measurements on bottom-up emissions, Journal of Geophysical Research-Atmospheres, 116, 10.1029/2011jd016575, 2011.

Wang, X., Wang, Y., Hao, J., Kondo, Y., Irwin, M., Munger, J. W., and Zhao, Y.: Top-down estimate of China's black carbon emissions using surface observations: Sensitivity to observation representativeness and transport model error, Journal of Geophysical Research-Atmospheres, 118, 5781-5795, 10.1002/jgrd.50397, 2013.

Xia, Y., Zhao, Y., and Nielsen, C. P.: Benefits of of China's efforts in gaseous pollutant control indicated by the bottom-up emissions and satellite observations 2000-2014, Atmospheric Environment, 136, 43-53, 10.1016/j.atmosenv.2016.04.013, 2016.

Xu, X., Wang, J., Henze, D. K., Qu, W., and Kopacz, M.: Constraints on aerosol sources using GEOS-Chem adjoint and MODIS radiances, and evaluation with multisensor (OMI, MISR) data, Journal of Geophysical Research-Atmospheres, 118, 10139-10139, 10.1002/jgrd.50784, 2013.

Yang, B., Zhang, Y., Qian, Y., Huang, A., and Yan, H.: Calibration of a convective parameterization scheme in the WRF model and its impact on the simulation of East Asian summer monsoon precipitation, Clim. Dyn., 44, 1661-1684, 10.1007/s00382-014-2118-4, 2014.

Yu, E., Wang, H., Gao, Y., and Sun, J.: Impacts of cumulus convective parameterization schemes on summer monsoon precipitation simulation over China, Acta Meteorologica Sinica, 25, 581-592, 10.1007/s13351-011-0504-y, 2011.

Zhang, L., Henze, D. K., Grell, G. A., Carmichael, G. R., Bousserez, N., Zhang, Q., Torres, O., Ahn, C., Lu, Z., Cao, J., and Mao, Y.: Constraining black carbon aerosol over Asia using OMI aerosol absorption optical depth and the adjoint of GEOS-Chem, Atmospheric Chemistry and Physics, 15, 10281-10308, 10.5194/acp-15-10281-2015, 2015.

Zhang, Q., Streets, D. G., Carmichael, G. R., He, K. B., Huo, H., Kannari, A., Klimont, Z., Park, I. S., Reddy, S., Fu, J. S., Chen, D., Duan, L., Lei, Y., Wang, L. T., and Yao, Z. L.: Asian emissions in 2006 for the NASA INTEX-B mission, Atmospheric Chemistry and Physics, 9, 5131-5153, 10.5194/acp-9-5131-2009, 2009.

Zhang, Y., Liu, P., Pun, B., and Seigneur, C.: A comprehensive performance evaluation of MM5-CMAQ for the Summer 1999 Southern Oxidants Study episode - Part I: Evaluation protocols, databases, and meteorological predictions, Atmospheric Environment, 40, 4825-4838, 10.1016/j.atmosenv.2005.12.043, 2006.

Zhao, Y., Zhang, J., and Nielsen, C. P.: The effects of energy paths and emission controls and standards on future trends in China's emissions of primary air pollutants, Atmospheric Chemistry and Physics, 14, 8849-8868, doi:10.5194/acp-14-8849-2014, 2014.

Zhao, Y., Zhang, J., and Nielsen, C. P.: The effects of recent control policies on trends in emissions of anthropogenic atmospheric pollutants and CO_2 in China, Atmospheric Chemistry and Physics, 13, 487-508, 10.5194/acp-13-487-2013, 2013.

Zheng, J., He, M., Shen, X., Yin, S., and Yuan, Z.: High resolution of black carbon and organic carbon emissions in the Pearl River Delta region, China, Science of the Total Environment, 438, 189-200, 10.1016/j.scitotenv.2012.08.068, 2012.

Zhou, Y., Zhao, Y., Mao, P., Zhang, Q., Zhang, J., Qiu, L., and Yang, Y.: Development of a high-resolution emission inventory and its evaluation and application through air quality modeling for Jiangsu Province, China, Atmospheric Chemistry and Physics, 17, 211-233, 10.5194/acp-17-211-2017, 2017.

Atmos. Chem. Phys. Discuss., https://doi.org/10.5194/acp-2018-984
Manuscript under review for journal Atmos. Chem. Phys.
Discussion started: 4 October 2018

Figure captions

Figure 1. Modeling domain and locations of two observation sites and three meteorological stations.

Figure 2. The monthly (left axis) and annual emissions (right axis) by sector for southern Jiangsu 2015 in JS-prior and JS-posterior (unit: Gg).

Figure 3. The seasonal variation of BC emissions by source (a) and total emissions (b) in JS-prior, JS-posterior and MEIC-prior.

Figure 4. The observed and simulated hourly BC concentrations at NJU using JS-prior and JS-posterior for January (a), April (b), July (c) and October (d) in 2015.

Figure 5. The same as Figure 4 but at PAES.

Figure 6. BC emission estimates by source of JS-prior, MEIC-prior, JS-posterior, and MEIC-posterior in April 2015 in southern Jiangsu.

Figure 7. The spatial distributions of the deviations (JS-MEIC) between JS-prior and MEIC-prior (a) and those between JS-posterior and MEIC-posterior (b).

Figure 8. The scatter plots of the simulated BC concentrations using JS inventories versus those using MEIC at NJU (a) and PAES (b).

Figure 9. The correlation between the simulated BC concentrations with JS-prior and those with doubled (a and c) or halved emissions in JS-prior (b and d) in July (a and b) and October (c and d) at NJU. $F_{emis.}$ and $F_{conc.}$ indicate respectively the fraction of changed emissions and that of changed simulated monthly average concentrations between sensitivity and base simulation (Scenario B). ΔE and ΔC indicated the change in emissions and that in simulated monthly average concentrations, respectively.

Figure 10. The same as Figure 9 but at PAES.

Atmos. Chem. Phys. Discuss., https://doi.org/10.5194/acp-2018-984
Manuscript under review for journal Atmos. Chem. Phys.
Discussion started: 4 October 2018

Figure 11. The ⊿BC/⊿CO ratio at NJU (a) and PAES (b) separated by different accumulated precipitation along the back trajectories during 48 h. The number of remaining data points is also given.

Figure 12. The wet deposition in Case 6 and accumulated precipitation in Case 7 at NJU (a) and PAES (b). The number of remaining data points is also given.

Atmos. Chem. Phys. Discuss., https://doi.org/10.5194/acp-2018-984
Manuscript under review for journal Atmos. Chem. Phys.
Discussion started: 4 October 2018

Atmospheric Chemistry and Physics
Discussions
Open Access

974 # Tables

975 **Table 1. The scaling factors and statistical indicators from the multiple**
976 **regression model for estimation of JS-posterior.**

Month	Sector	Scaling factor	t[a]	Sig.[b]	VIF[c]	Sig.[d]
January	Industry (β_2)	0.42	2.65	0.01	1.76	0.00
	Residential (β_3)	1.31	3.67	0.00	2.37	
	Transportation (β_4)	0.79	2.23	0.03	2.72	
April	Industry (β_2)	0.22	0.96	0.34	2.65	0.00
	Residential (β_3)	0.58	1.63	0.11	4.62	
	Transportation (β_4)	0.67	2.21	0.03	4.19	
July	Industry (β_2)	0.35	3.09	0.00	2.09	0.00
	Residential (β_3)	0.39	0.95	0.34	2.95	
	Transportation (β_4)	0.55	2.20	0.03	3.46	
October	Industry (β_2)	0.34	1.92	0.06	1.53	0.00
	Residential (β_3)	1.52	4.12	0.00	2.20	
	Transportation (β_4)	0.74	2.80	0.01	2.65	

977 Note: The criteria for the statistical significance of the model: a: t>2, b: Sig.<0.05, and
978 c: VIF<10, d: the overall significance.

Table 2. Statistical indicators for observed and simulated BC concentrations using JS-prior and JS-posterior at NJU and PAES.

Site	Parameter	January		April		July		October		Annual	
		JS-prior	JS-posterior	JS-prior	JS-posterior	JS-prior	JS-posterior	JS-prior	JS-posterior	JS-prior	JS-posterior
NJU	Average SIM (μg/m^3)	5.97	5.50	2.38	1.82	1.99	1.29	2.80	2.42	3.44	2.82
	Average OBS (μg/m^3)	5.44	5.44	2.69	2.69	2.65	2.65	3.96	3.96	3.83	3.83
	NMB (%)	8.35	-0.08	-16.02	-32.40	-23.09	-51.32	-29.20	-39.01	-10.16	26.43
	NME (%)	37.83	35.54	42.31	38.61	49.62	57.49	40.52	43.06	41.15	44.16
	R	0.67	0.66	0.34	0.43	0.36	0.31	0.42	0.48	0.67	0.69
PAES	Average SIM (μg/m^3)	6.46	5.91	2.98	1.95	2.61	1.63	3.19	2.88	3.39	2.57
	Average OBS (μg/m^3)	2.80	2.80	1.70	1.70	1.51	1.51	3.62	3.62	2.48	2.48
	NMB (%)	151.93	134.59	61.57	14.73	72.17	8.28	-12.01	-20.48	36.67	3.54
	NME (%)	155.53	139.50	73.18	42.87	92.74	42.37	43.10	40.80	72.00	57.55
	R	0.38	0.38	0.64	0.53	0.35	0.37	0.57	0.72	0.38	0.45

Note: SIM and OBS indicated the results from simulation and observation, respectively. NMB and NME were calculated using following equations (P and O indicated the results from modeling prediction and observation, respectively):

$$NMB = \frac{\sum_{i=1}^{n}(P_i - O_i)}{\sum_{i=1}^{n} O_i} \times 100\% ; . NME = \frac{\sum_{i=1}^{n}|P_i - O_i|}{\sum_{i=1}^{n} O_i} \times 100\%$$

Atmospheric Chemistry and Physics
Open Access
Discussions

Atmos. Chem. Phys. Discuss., https://doi.org/10.5194/acp-2018-984
Manuscript under review for journal Atmos. Chem. Phys.
Discussion started: 4 October 2018

Table 3. Statistical indicators for observed and simulated BC concentrations in different cases in April 2015 at NJU and PAES.

Site	Parameter	Scenario B	Case1	Case2	Case3	Case4	Case5
	Average SIM (μg/m^3)	2.38	1.82	2.27	2.06	2.49	1.78
	Average OBS (μg/m^3)	2.69	2.69	2.69	2.69	2.69	2.69
NJU	NMB (%)	-16.02	-32.40	-21.59	-23.50	-7.46	-33.95
	NME (%)	42.31	38.61	32.47	32.64	41.58	38.94
	R	0.34	0.43	0.49	0.49	0.40	0.46
	Average SIM (μg/m^3)	2.98	1.95	2.45	2.01	5.13	2.29
	Average OBS (μg/m^3)	1.70	1.70	1.70	1.70	1.70	1.70
PAES	NMB (%)	61.57	14.73	49.86	18.02	201.35	34.71
	NME (%)	73.18	42.87	61.59	39.62	201.56	47.73
	R	0.64	0.53	0.63	0.66	0.65	0.59

985 **Table 4. The scaling factors and statistical indicators from the multiple**
986 **regression model in Case 3.**

Site	Sector	Scaling factor	t	Sig.	VIF
NJU	Industry (β_2)	0.42	1.71	0.09	2.03
	Residential (β_3)	0.95	2.50	0.01	2.52
	Transportation (β_4)	0.65	2.13	0.03	2.66
PAES	Industry (β_2)	0.19	3.46	0.00	1.44
	Residential (β_3)	0.36	1.89	0.06	1.44
	Transportation(β_4)	0.65	-	-	-

Atmos. Chem. Phys. Discuss., https://doi.org/10.5194/acp-2018-984
Manuscript under review for journal Atmos. Chem. Phys.
Discussion started: 4 October 2018

Atmospheric Chemistry and Physics Discussions

Table 5. BC emissions from Nanjing and Suzhou–Wuxi–Changzhou-Zhenjiang city cluster in different cases in April 2015 (Gg).

Case	Sector	Nanjing	Suzhou–Wuxi–Changzhou -Zhenjiang	Southern Jiangsu
Scenario B	Power	0	0.01	0.01
	Industry	0.21	1.13	1.34
	Residential	0.08	0.24	0.32
	Transportation	0.12	0.30	0.42
	Total	0.41	1.68	2.09
Case 1	Power	0	0.01	0.01
	Industry	0.05	0.25	0.30
	Residential	0.04	0.14	0.19
	Transportation	0.08	0.20	0.28
	Total	0.17	0.60	0.78
Case 2	Power	0	0.01	0.01
	Industry	0.09	0.47	0.56
	Residential	0.07	0.23	0.30
	Transportation	0.08	0.20	0.27
	Total	0.24	0.91	1.14
Case 3	Power	0	0.01	0.01
	Industry	0.04	0.47	0.51
	Residential	0.03	0.23	0.26
	Transportation	0.08	0.20	0.27
	Total	0.15	0.90	1.05

Atmos. Chem. Phys. Discuss., https://doi.org/10.5194/acp-2018-984
Manuscript under review for journal Atmos. Chem. Phys.
Discussion started: 4 October 2018

Atmospheric Chemistry and Physics Discussions

Table 6. The scaling factors and statistical indicators from the multiple regression model in Case 6.

Month	Sector	Scaling factor	t[a]	Sig.[b]	VIF[c]	Sig.[d]
January	Industry (β_2')	0.41	2.17	0.03	1.71	0.00
	Residential (β_3')	1.53	3.48	0.00	2.29	
	Transportation (β_4')	0.73	1.65	0.10	2.66	
April	Industry (β_2')	0.24	0.92	0.36	1.91	0.00
	Residential (β_3')	0.51	1.32	0.19	3.29	
	Transportation (β_4')	0.70	2.12	0.03	3.03	
July	Industry (β_2')	0.38	4.43	0.00	1.43	0.00
	Residential (β_3')	0.34	0.82	0.41	2.52	
	Transportation (β_4')	0.74	3.55	0.00	2.25	
October	Industry (β_2')	0.33	1.00	0.32	1.44	0.00
	Residential (β_3')	1.36	2.61	0.01	1.86	
	Transportation (β_4')	0.72	1.89	0.06	2.02	

Note: The criteria for the statistical significance of the model: a: $t>2$, b: $Sig.<0.05$, and c: $VIF<10$, d: the overall significance.

Atmos. Chem. Phys. Discuss., https://doi.org/10.5194/acp-2018-984
Manuscript under review for journal Atmos. Chem. Phys.
Discussion started: 4 October 2018

994 **Table 7. The monthly and annual emissions by sector for southern Jiangsu 2015 in Case 6 (unit: Gg) and the relative deviation**
995 **compared to Case 1 (RD: Case 6–Case 1)/Case 1).**

	January		April		July		October		Annual	
	Case 6	RD	Case 6	RD	Case 6	RD	Case 6	RD	Case 6	RD
Power	0.0	0.0%	0.0	0.0%	0.0	0.0%	0.0	0.0%	0.0	0.0%
Industry	0.6	-2.4%	0.3	9.9%	0.6	9.2%	0.5	-0.3%	6.0	3.1%
Residential	0.5	16.7%	0.2	-13.1%	0.1	-13.7%	0.4	-10.2%	3.6	-0.6%
Transportation	0.3	-8.2%	0.3	4.3%	0.4	34.4%	0.3	-3.0%	3.9	5.4%
Sum	1.4	2.4%	0.8	2.3%	1.1	13.6%	1.2	-4.2%	13.5	2.6%

996
997
998
999

Atmos. Chem. Phys. Discuss., https://doi.org/10.5194/acp-2018-984
Manuscript under review for journal Atmos. Chem. Phys.
Discussion started: 4 October 2018

Table 8. Statistical indicators for the observed and simulated BC concentrations in July 2015 at NJU and PAES in Case 6 and Case 7.

	Parameter	Case 6	Case 7
NJU	Average SIM (μg/m^3)	1.40	1.41
	Average OBS (μg/m^3)	2.65	2.65
	NMB (%)	-47.41	-46.72
	NME (%)	54.88	54.44
	R	0.33	0.33
PAES	Average SIM (μg/m^3)	1.76	1.76
	Average OBS (μg/m^3)	1.51	1.51
	NMB (%)	16.87	16.65
	NME (%)	44.46	42.71
	R	0.36	0.39

Note: SIM and OBS indicated the results from simulation and observation, respectively. NMB and NME were calculated using following equations (P and O indicated the results from modeling prediction and observation, respectively):

$$NMB = \frac{\sum_{i=1}^{n}(P_i - O_i)}{\sum_{i=1}^{n} O_i} \times 100\% \quad ; \quad NME = \frac{\sum_{i=1}^{n}|P_i - O_i|}{\sum_{i=1}^{n} O_i} \times 100\%$$

Table 9. The scaling factors and statistical indicators from the multiple regression model in Case 7. The emissions by sector for southern Jiangsu 2015 July in Case 7 (unit: Gg) and the relative deviations (RD) compared to Case 1 (RD: Case 7–Case 1)/Case 1) are also shown in table.

Sector	Scaling factor	t[a]	Sig.[b]	VIF[c]	Sig.[d]	Emissions	RD
Power						0.0	0.0%
Industry (β_2')	0.38	2.38	0.02	1.31		0.5	9.5%
Residential (β_3')	0.31	0.31	0.75	2.31	0.00	0.1	-20.6%
Transportation (β_4')	0.75	1.8	0.07	1.95		0.4	36.4%
Sum						1.0	13.4%

Note: The criteria for the statistical significance of the model: a: t>2, b: Sig.<0.05, and c: VIF<10, d: the overall significance.

Figure 1

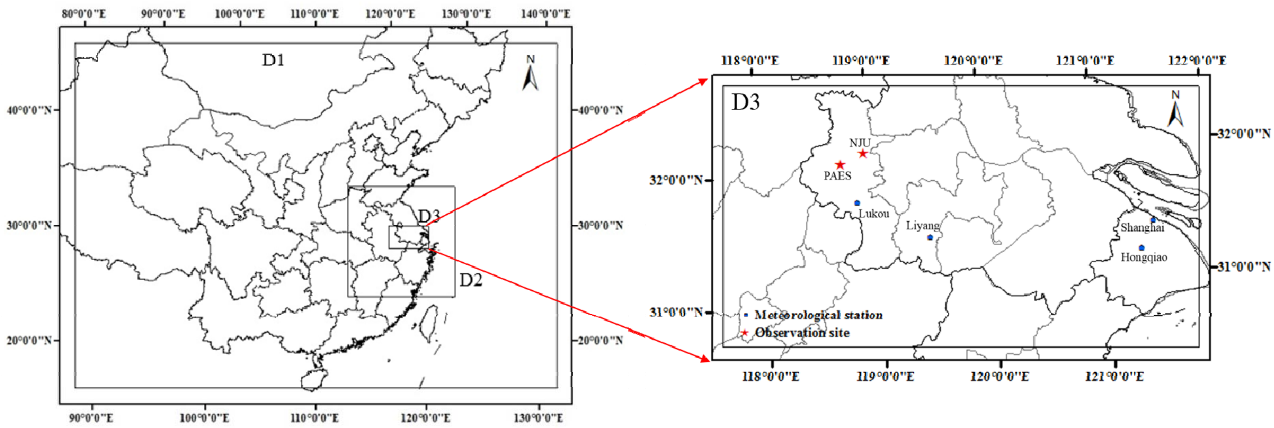
D1
D2
D3
N
NJU
PAES
Lukou
Liyang
Shanghai
Hongqiao
Meteorological station
Observation site

Atmos. Chem. Phys. Discuss., https://doi.org/10.5194/acp-2018-984
Manuscript under review for journal Atmos. Chem. Phys.
Discussion started: 4 October 2018

Atmospheric Chemistry and Physics
Open Access
Discussions

Figure 2

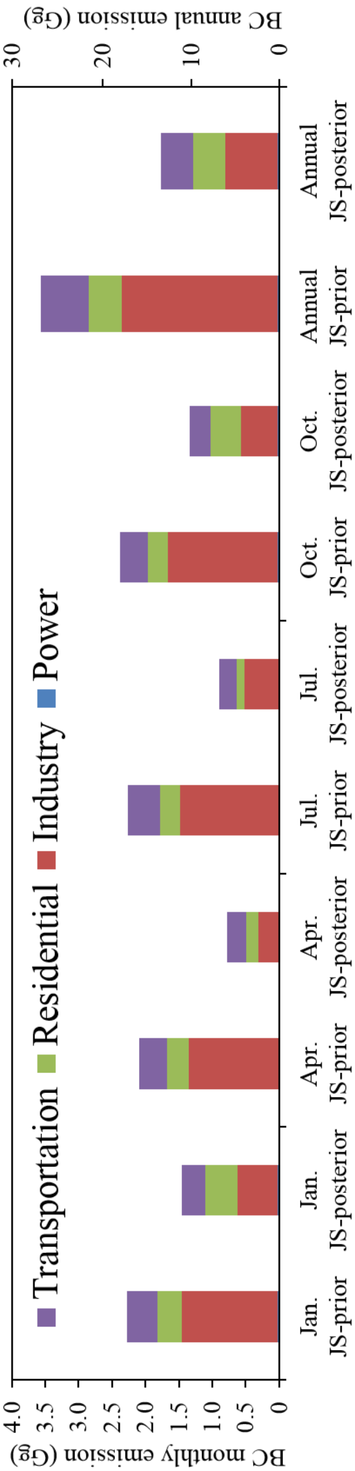

Atmos. Chem. Phys. Discuss., https://doi.org/10.5194/acp-2018-984
Manuscript under review for journal Atmos. Chem. Phys.
Discussion started: 4 October 2018

Figure 3

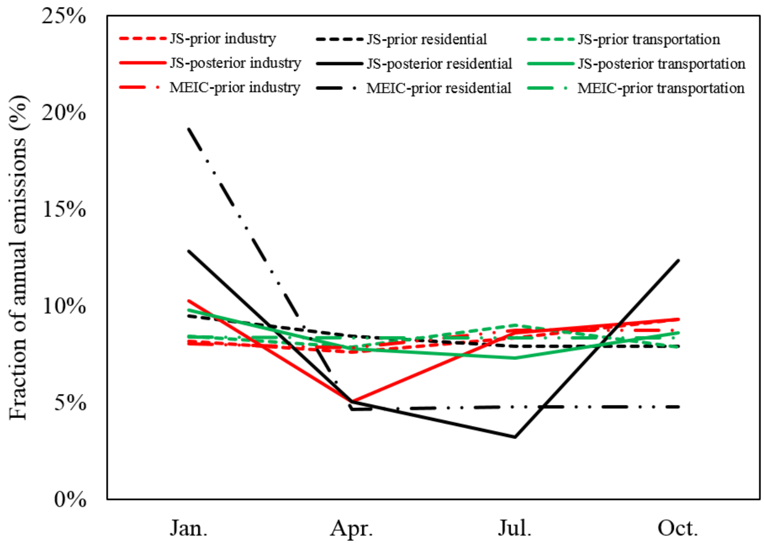

(a)

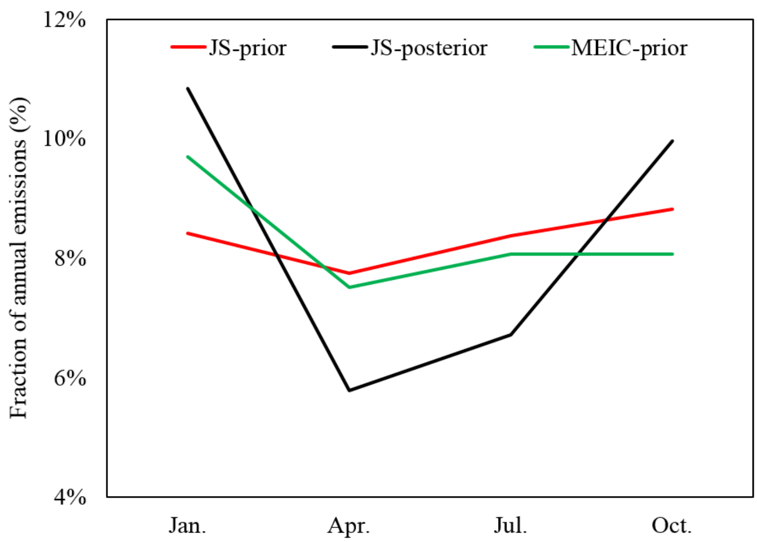

(b)

Atmos. Chem. Phys. Discuss., https://doi.org/10.5194/acp-2018-984
Manuscript under review for journal Atmos. Chem. Phys.
Discussion started: 4 October 2018

Atmospheric Chemistry and Physics
Open Access
Discussions

Figure 4

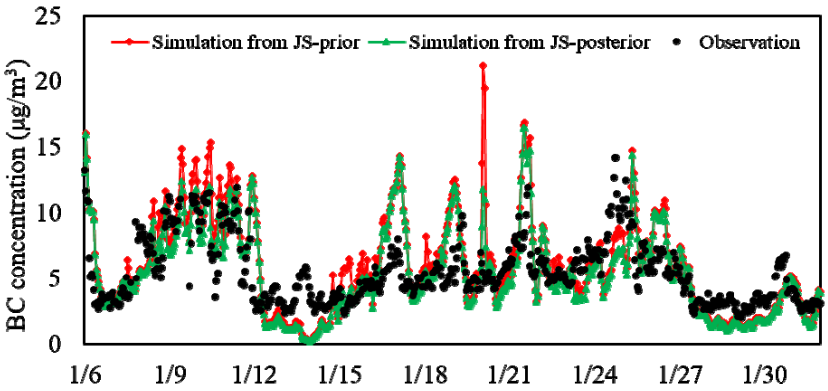

(a)

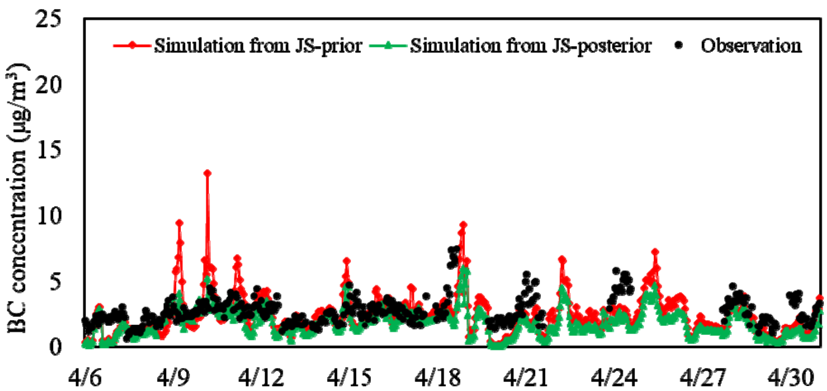

(b)

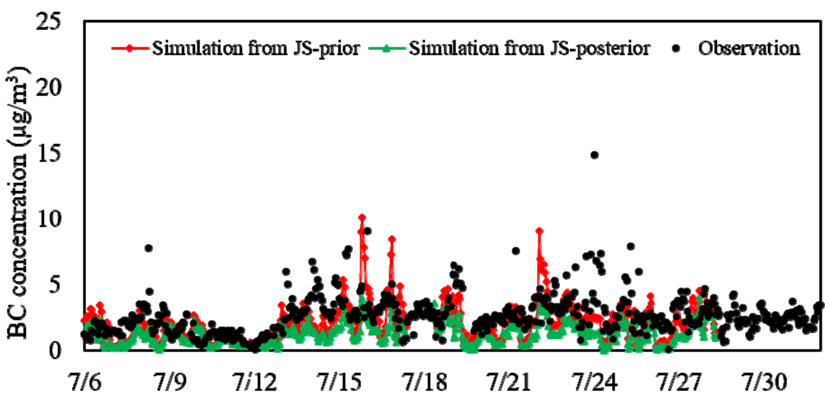

(c)

Atmos. Chem. Phys. Discuss., https://doi.org/10.5194/acp-2018-984
Manuscript under review for journal Atmos. Chem. Phys.
Discussion started: 4 October 2018

Atmospheric Chemistry and Physics Discussions
Open Access

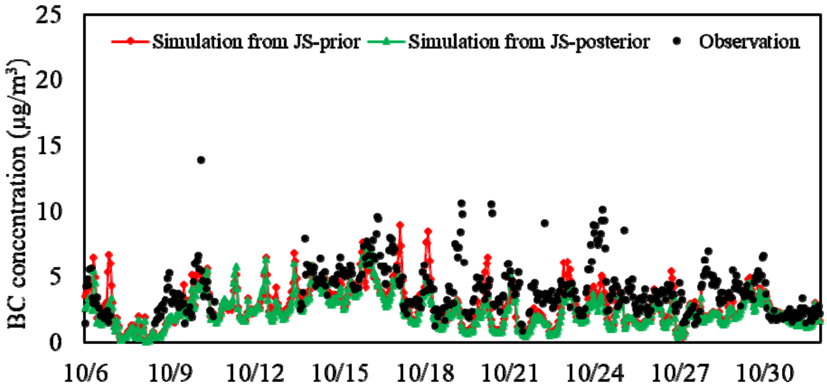

(d)

Atmos. Chem. Phys. Discuss., https://doi.org/10.5194/acp-2018-984
Manuscript under review for journal Atmos. Chem. Phys.
Discussion started: 4 October 2018

Atmospheric Chemistry and Physics
Discussions

1052 **Figure 5**

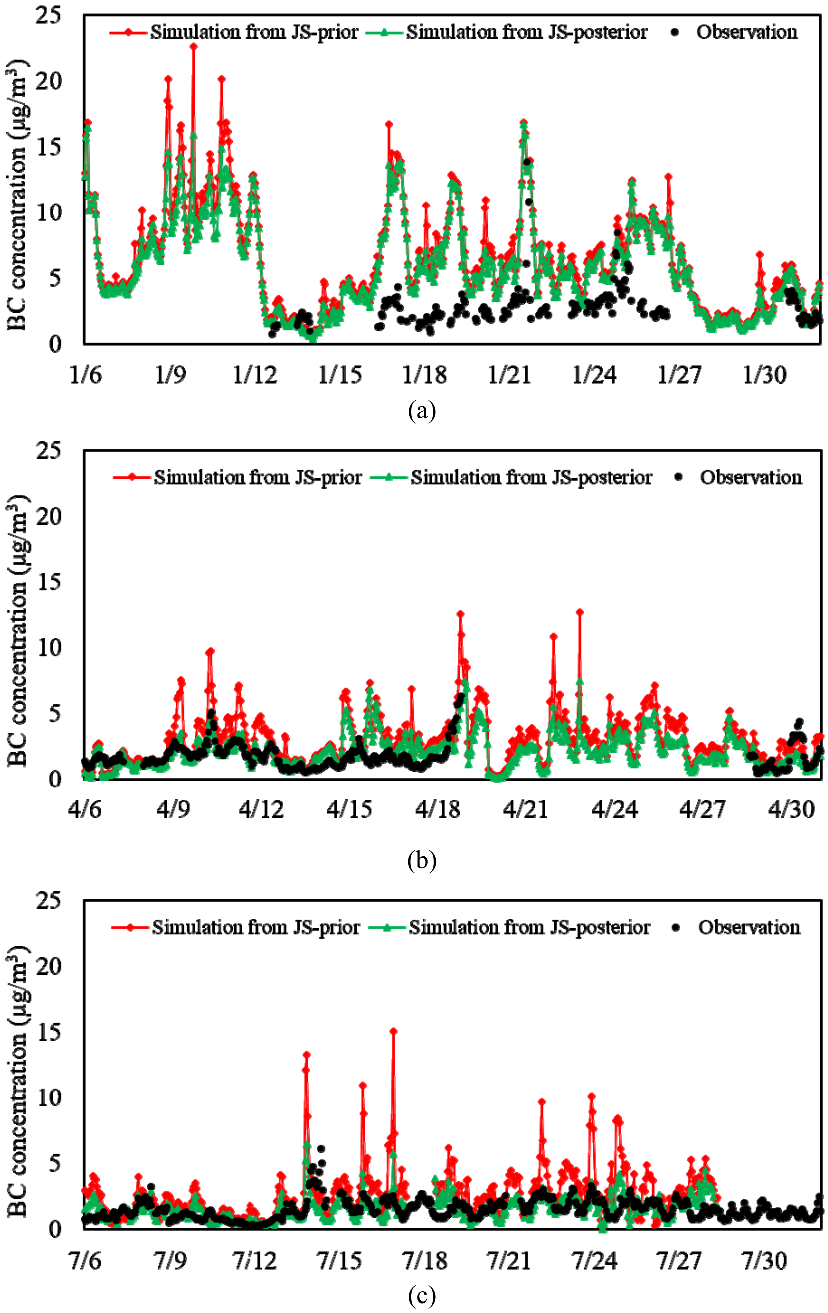

Atmos. Chem. Phys. Discuss., https://doi.org/10.5194/acp-2018-984
Manuscript under review for journal Atmos. Chem. Phys.
Discussion started: 4 October 2018

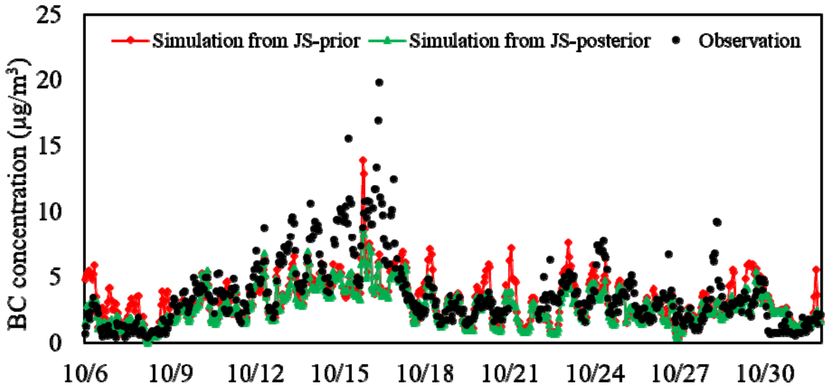

(d)

1053

Atmos. Chem. Phys. Discuss., https://doi.org/10.5194/acp-2018-984
Manuscript under review for journal Atmos. Chem. Phys.
Discussion started: 4 October 2018

1054 **Figure 6**

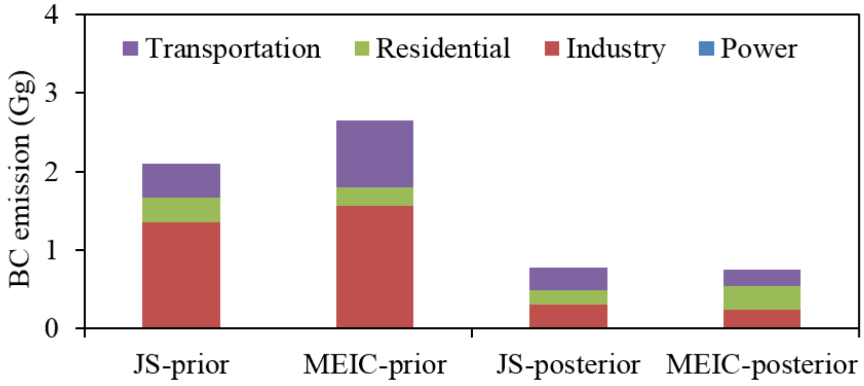

1055

1056 **Figure 7**

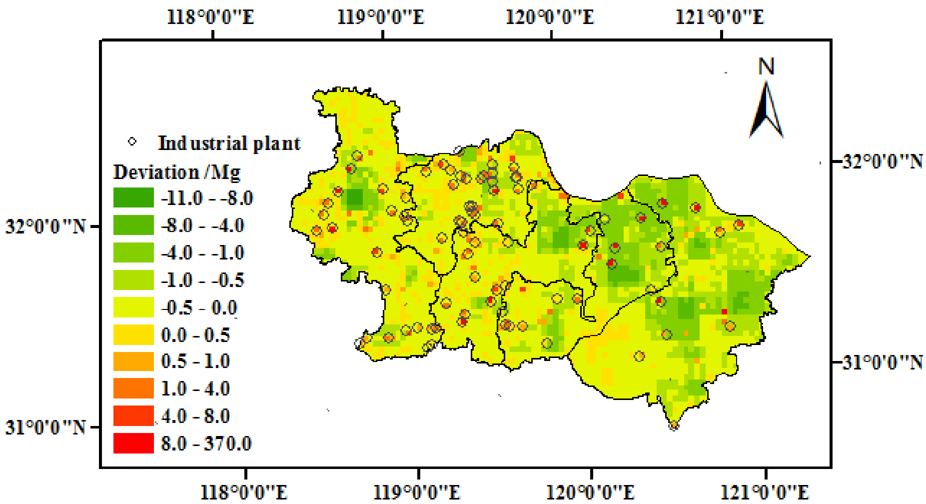

(a)

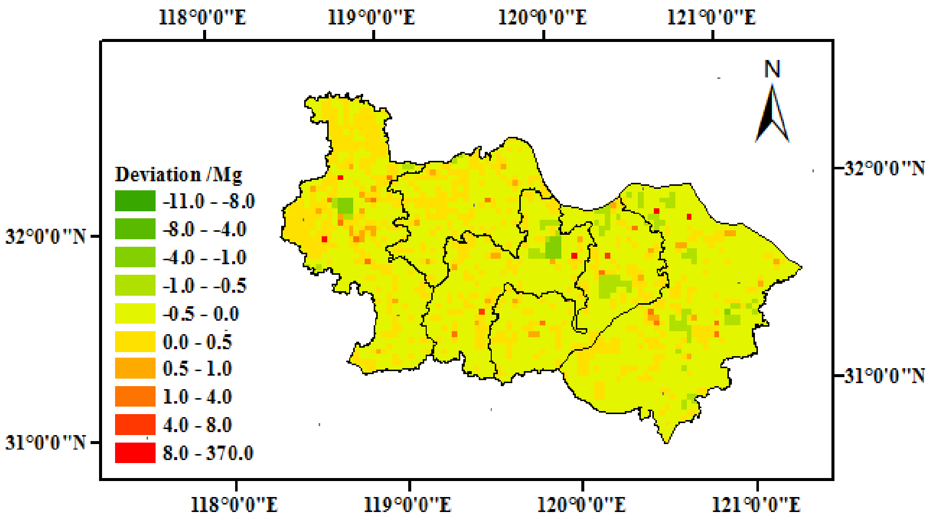

(b)

1057

Atmos. Chem. Phys. Discuss., https://doi.org/10.5194/acp-2018-984
Manuscript under review for journal Atmos. Chem. Phys.
Discussion started: 4 October 2018

Atmospheric Chemistry and Physics
Open Access
EGU
Discussions

Figure 8

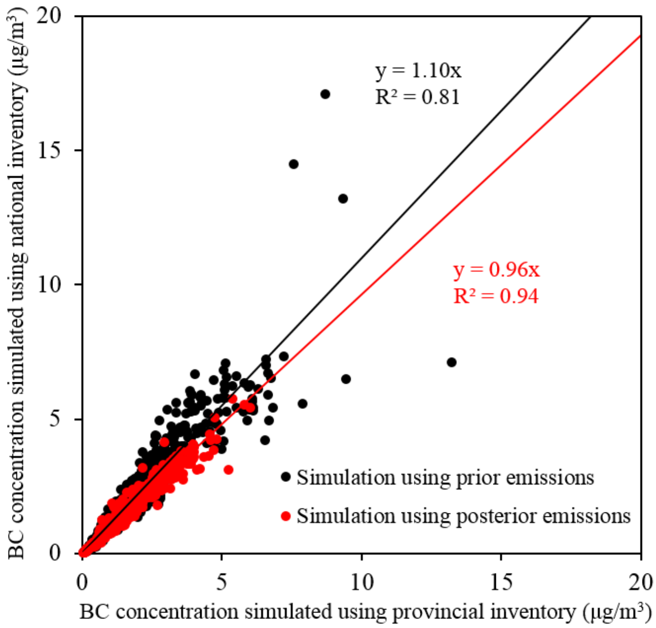

(a)

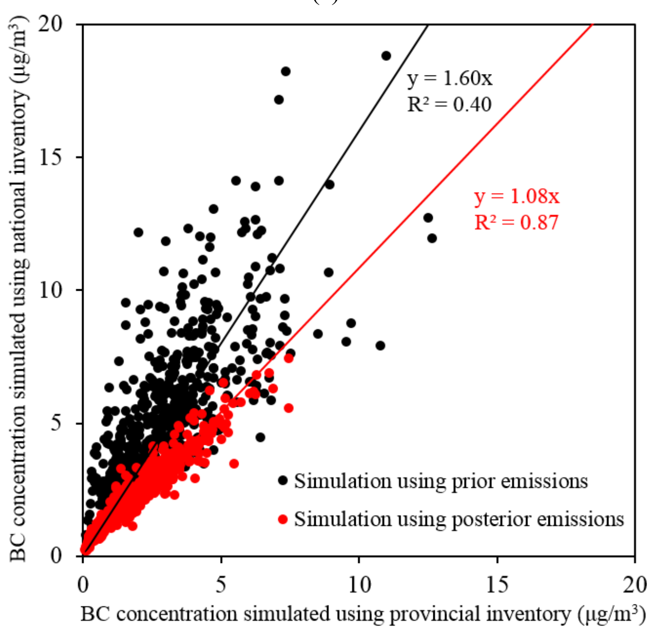

(b)

Atmos. Chem. Phys. Discuss., https://doi.org/10.5194/acp-2018-984
Manuscript under review for journal Atmos. Chem. Phys.
Discussion started: 4 October 2018

Figure 9

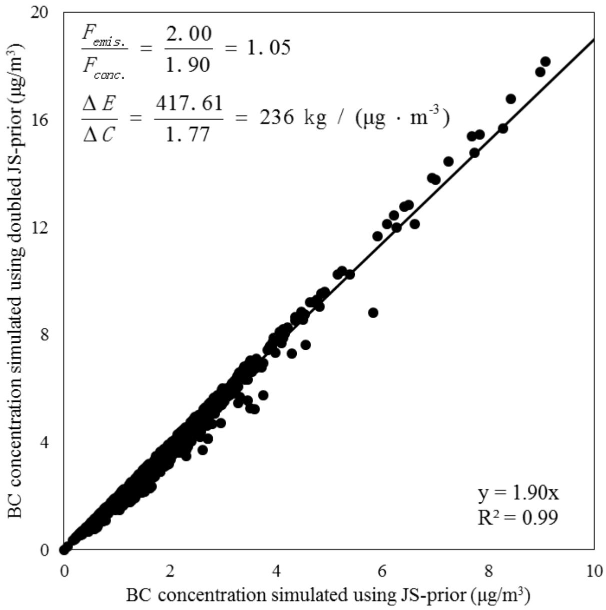

(a)

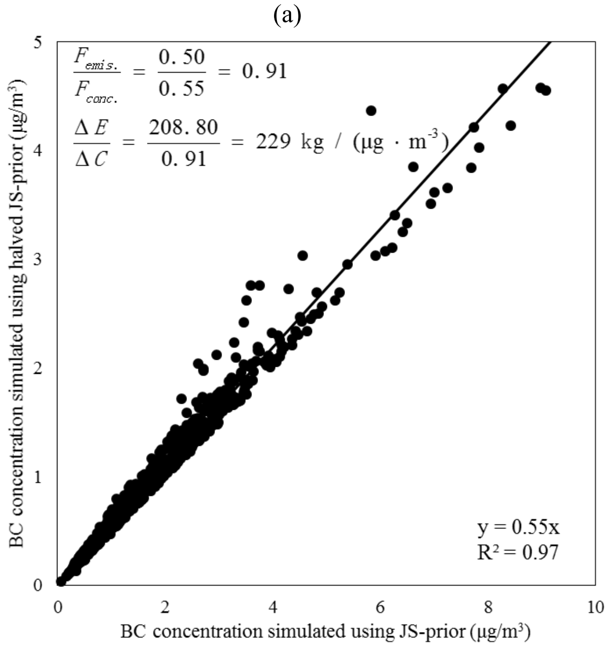

(b)

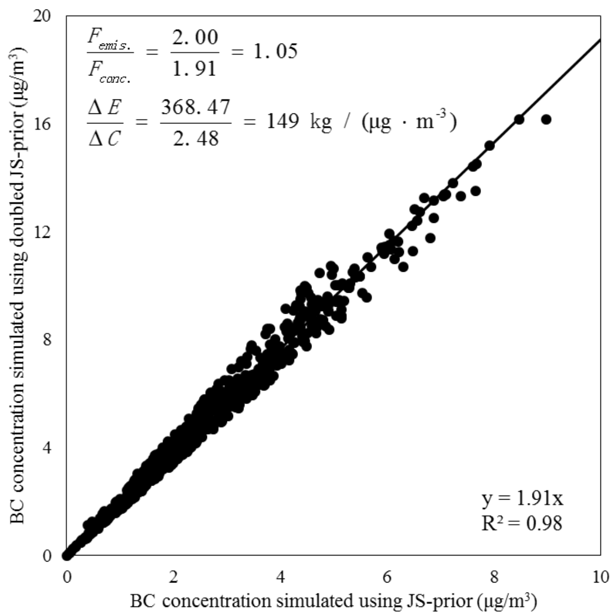
$\frac{F_{emis.}}{F_{conc.}} = \frac{2.00}{1.91} = 1.05$
$\frac{\Delta E}{\Delta C} = \frac{368.47}{2.48} = 149$ kg / (μg · m^{-3})
y = 1.91x
R^2 = 0.98
BC concentration simulated using doubled JS-prior (μg/m^3)
BC concentration simulated using JS-prior (μg/m^3)

(c)

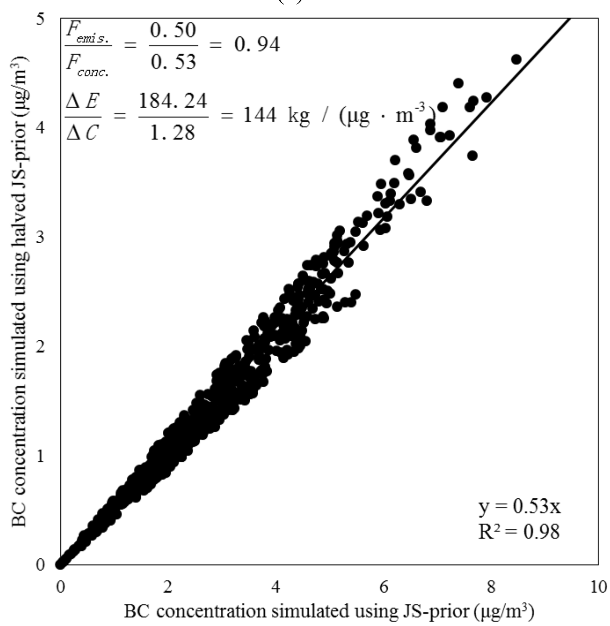
$\frac{F_{emis.}}{F_{conc.}} = \frac{0.50}{0.53} = 0.94$
$\frac{\Delta E}{\Delta C} = \frac{184.24}{1.28} = 144$ kg / (μg · m^{-3})
y = 0.53x
R^2 = 0.98
BC concentration simulated using halved JS-prior (μg/m^3)
BC concentration simulated using JS-prior (μg/m^3)

(d)

1062

Atmos. Chem. Phys. Discuss., https://doi.org/10.5194/acp-2018-984
Manuscript under review for journal Atmos. Chem. Phys.
Discussion started: 4 October 2018

1063 **Figure 10**

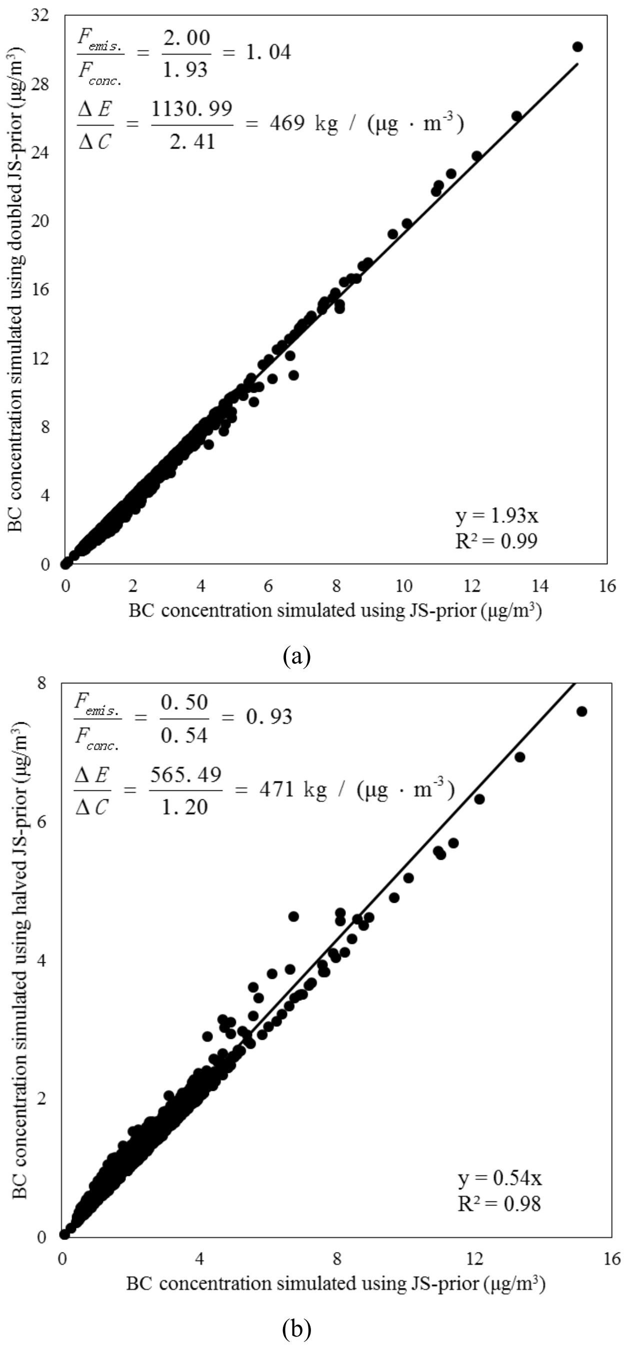

1064

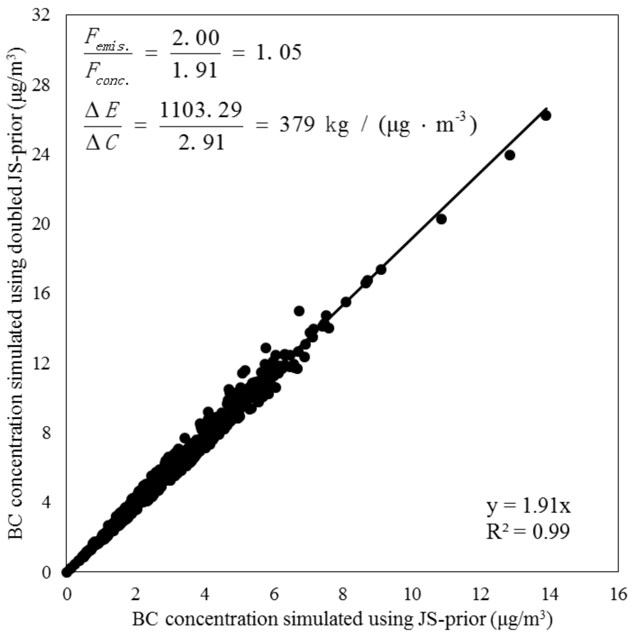
$\frac{F_{emis.}}{F_{conc.}} = \frac{2.00}{1.91} = 1.05$
$\frac{\Delta E}{\Delta C} = \frac{1103.29}{2.91} = 379$ kg / (μg · m^{-3})
y = 1.91x
R^2 = 0.99
BC concentration simulated using doubled JS-prior (μg/m^3)
BC concentration simulated using JS-prior (μg/m^3)
0
4
8
12
16
20
24
28
32
2
6
10
14

(c)

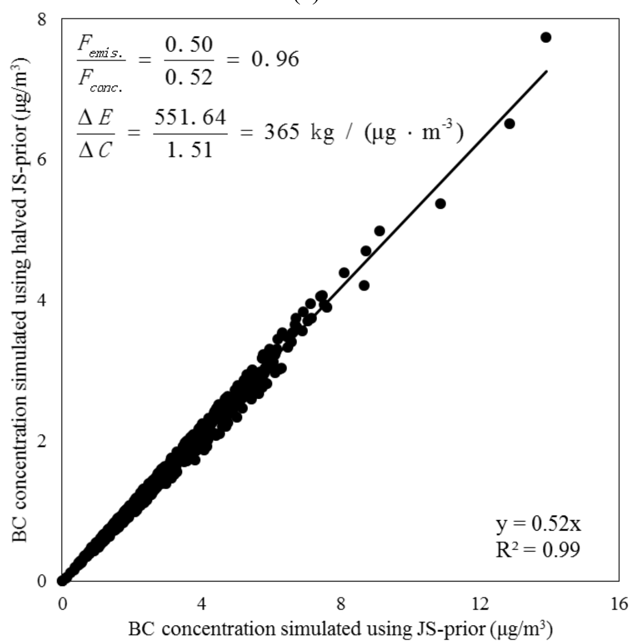
$\frac{F_{emis.}}{F_{conc.}} = \frac{0.50}{0.52} = 0.96$
$\frac{\Delta E}{\Delta C} = \frac{551.64}{1.51} = 365$ kg / (μg · m^{-3})
y = 0.52x
R^2 = 0.99
BC concentration simulated using halved JS-prior (μg/m^3)
BC concentration simulated using JS-prior (μg/m^3)
0
2
4
6
8
12
16

(d)

1068 **Figure 11**

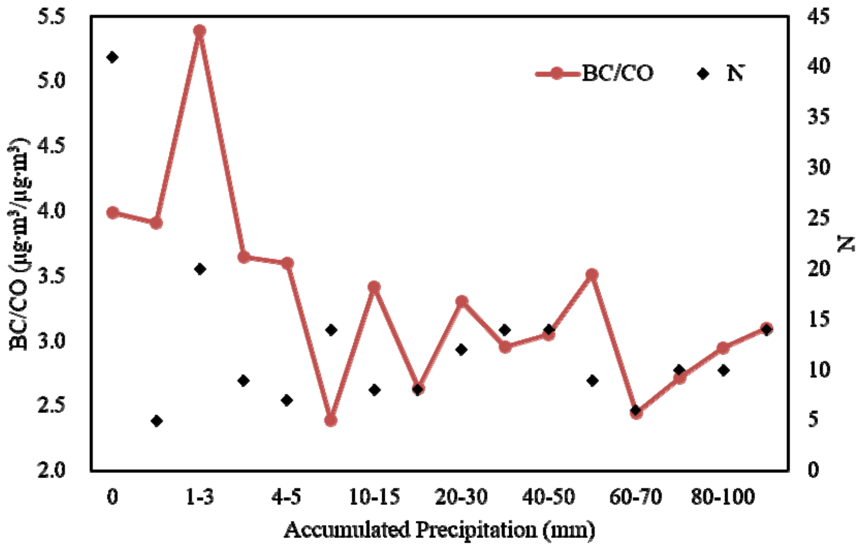

(a)

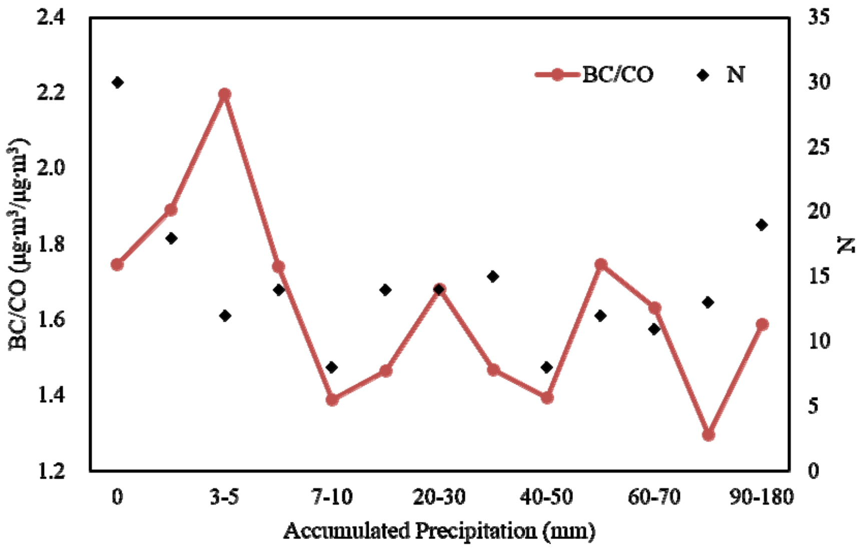

(b)

1069
1070
1071
1072

Atmos. Chem. Phys. Discuss., https://doi.org/10.5194/acp-2018-984
Manuscript under review for journal Atmos. Chem. Phys.
Discussion started: 4 October 2018

Figure 12

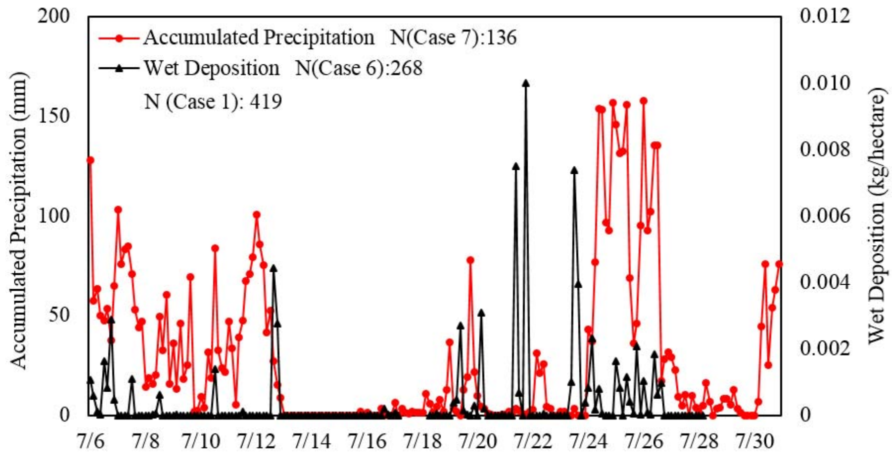

(a)

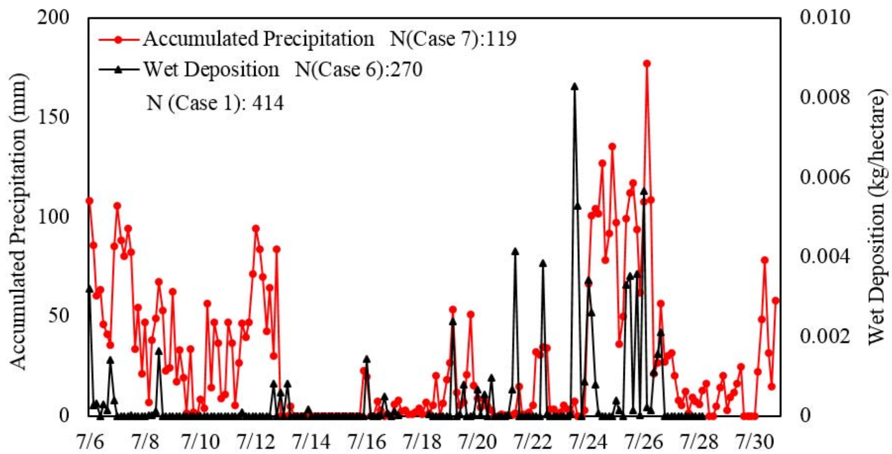

(b)